

**Episodicity of Mesozoic terrane accretion along the Pacific margin of
Gondwana: implications for superplume–plate interactions.**

A.P.M. VAUGHAN & R.A. LIVERMORE

*British Antarctic Survey, High Cross, Madingley Rd, Cambridge, CB3 0ET, UK
(email: a.vaughan@bas.ac.uk)*

No of words in text: 11,597

No of references: 337

No of tables: 2

No of Figures: 5

Running Title: Episodicity of terrane accretion

Abstract: A review of evidence for deformation and terrane accretion on the Late Triassic–Early Jurassic margins of Pangea and the mid-Cretaceous margins of the palaeo-Pacific ocean shows that deformation was global and synchronous with probable superplume events. Late Triassic–Early Jurassic deformation appears to be concentrated in the period 202–197 Ma and was coeval with eruption of the Central Atlantic Magmatic Province, onset of Pangea break-up, a period of extended normal magnetic polarity and a major mass extinction event, all possible expressions of a superplume event. Mid-Cretaceous deformation occurred in two brief periods, the first from approximately 116 to 110 Ma in the west palaeo-Pacific and the second from roughly 105 to 99 Ma in the east palaeo-Pacific, with both events possibly represented in northeast Siberia. This deformation was coeval with eruption of major oceanic plateaus, core-complex formation and rifting of New Zealand from Gondwana, the Cretaceous normal polarity epoch, and a major radiation of flowering plants and several animal groups, all linked with the mid-Cretaceous superplume event. A simple unifying mechanism is presented suggesting that large continental or oceanic plates, when impacted by a superplume, tend to break-up/reorganize, associated with gravitational spreading away from a broad, thermally generated topographic high and with a resulting short-lived pulse of plate-marginal deformation and terrane accretion.

Long-term episodicity of geological activity, i.e. variations of intensity or style with time but not necessarily to any particular periodicity, has been proposed for many processes, including aspects of magmatism (Prokoph *et al.* 2004) and tectonism (Condie 1998), from the Early Archaean to the present era. Generally the origin of episodicity has been attributed to mantle thermal behaviour. This is either as gradual

changes associated with the growth and fragmentation of supercontinents, the so-called Wilson Cycle, as a result of processes such as thermal shielding (Condie 2002), or more catastrophic, non-linear events, referred to as superplumes (Abbott & Isley 2002; Condie 1998; Larson 1991b) or mantle avalanches (Butler & Peltier 1997; Machetel 2003; Solheim & Peltier 1994). In this paper, we review the evidence for timing and nature of two episodes of Mesozoic terrane accretion and deformation (summarized in Tables 1 and 2). We propose that these were superplume-driven and we present a unifying mechanism and conceptual model for the interaction between large plates and superplume arrival from depth, focussing on deformation on the Gondwana/Pangaea margin during the Late Triassic–Early Jurassic and deformation on the margin of the palaeo-Pacific basin during the mid-Cretaceous. Both mid-Cretaceous and Late Triassic–Early Jurassic deformation events were temporally associated with a short-term global increase in the rate of ophiolite obduction (Vaughan & Scarrow 2003), and were associated with major, concentrated magmatic episodes (e.g., Larson 1997; Riley *et al.* 2004), changes in geomagnetic field behaviour (Biggin & Thomas 2003), and large-scale environmental perturbation (Hesselbo *et al.* 2002; Larson & Erba 1999). Time and timing is obviously very important, particularly when relating event chronologies determined from the stratigraphic record with those determined radiometrically. For consistency, all chronostratigraphic series and stage range and boundary ages are taken from the International Commission on Stratigraphy timescale published by Gradstein *et al.* (2004).

The two enigmatic orogenic events under consideration here are well-represented in rocks on the Pacific margin of Gondwana during the Mesozoic. The

Late Triassic–Early Jurassic event is called the Peninsula Orogeny in West Antarctica (Miller 1983) and the Rangitata I Orogeny in New Zealand (Bradshaw *et al.* 1981); the mid-Cretaceous event is called the Palmer Land event in the Antarctic Peninsula region (Kellogg & Rowley 1989; redated by Vaughan *et al.* 2002b) and the Rangitata II Orogeny in New Zealand (Bradshaw *et al.* 1981). Below we illustrate the global extent of deformation associated with these events. The Late Triassic–Early Jurassic event is widely developed in accretionary complex rocks that now sit outboard of rocks characteristic of continental Gondwana, and has recently been tentatively identified in Lower Palaeozoic rocks of the Pensacola Mountains (Curtis 2002). The deformation episode, which is found in Gondwana-margin rocks from New Zealand, Antarctica and South America, is particularly significant because it appears to have been active just prior to, or during, the earliest stages of Gondwana break-up. Suggested causes for the mountain-building event have varied widely, from Late Permian to mid-Jurassic dextral transpression and terrane collision (Martin *et al.* 1999), earliest Jurassic to early mid-Jurassic sinistral transpression (Scheuber & Gonzalez 1999), thermal uplift associated with the break-up of Gondwana (Dalziel 1982), a terrane–accretionary complex collision event (Bradshaw *et al.* 1981), or episodic accretionary complex activity (Thomson & Herve 2002). Aptian to Albian mid-Cretaceous tectonism widely affected rocks around the margin of the Pacific basin (Vaughan 1995) (Fig. 2), and is well-developed in all terranes of the Antarctic Peninsula where it is reasonably well dated to have occurred between ~107 Ma and ~103 Ma (Vaughan *et al.* 2002a; Vaughan *et al.* 2002b).

Distribution of Late Triassic–Early Jurassic deformation in Pangaea

Antarctica

The Peninsula Orogeny (Miller 1983; reassessed by Storey *et al.* 1987) of West Antarctica was recognized to be an orogenic event that post-dated the Late Palaeozoic, Gondwanian orogeny (Curtis 2001), affecting Late Palaeozoic and Mesozoic accretionary complex rocks such as the LeMay Group of Alexander Island (AI: Fig. 1) (Burn 1984; Tranter 1987) and Trinity Peninsula Group of Graham Land (TP: Fig. 1) (Aitkenhead 1975; Smellie 1981). Deformed accretionary complex rocks of the Western Domain (Vaughan & Storey 2000), LeMay Group in eastern Alexander Island are overlain by Bathonian (168–165 Ma) sediments of the Fossil Bluff Group (Doubleday *et al.* 1993). Dated LeMay Group rocks range in age from mid-Cretaceous in the west (Holdsworth & Nell 1992) to Sinemurian (197–190 Ma) in the east (Thomson & Tranter 1986) and possibly older (Kelly *et al.* 2001), but, in the absence of detailed field data, deformation can only be placed at pre-Bathonian (~168 Ma). Permian–Triassic turbiditic rocks of the Trinity Peninsula Group show polyphase deformation at anchizonal and epizonal metamorphic grade (Smellie *et al.* 1996) prior to deposition of the Early to Middle Jurassic non-marine Botany Bay Group (Cantrill 2000). D₂ deformation, which probably corresponds to the Peninsula Orogeny, constitutes an episode of margin-parallel sinistral transpressional shear (A.P.M. Vaughan unpublished data). Deformation and metamorphism of accretionary complex metapelites and metagreywackes in the Scotia Complex (SC: Fig. 1) of the South Orkney Islands occurred in Early Jurassic times (200–176 Ma) (Trouw *et al.* 1997) and these rocks are overlain by the Early to Middle Jurassic Powell Island conglomerate (Cantrill 2000). In the Patuxent Range of the Pensacola Mountains, East Antarctica (PM: Fig. 1), a early Jurassic phase of deformation predates the

intrusion of 183 Ma lamprophyre dykes and involved an inferred vertical axis rotation of pre-existing, end-Cambrian Ross and Permo-Triassic Gondwanian orogeny structures with the localized development of a spaced foliation and mesoscale folding (Curtis 2002).

South America

The Duke of York flysch of the Madre de Dios accretionary complex and the accretionary, Chonos metamorphic complex of Patagonia (C/M: Fig. 1) both show a Late Triassic-Early Jurassic metamorphic event (Thomson & Herve 2002), between 234 and 198 Ma, affecting sediments with detrital age patterns indicating Middle Triassic to Early Jurassic deposition (Hervé & Fanning 2001; Hervé *et al.* 2003). In the Bolfin Complex of the north Chilean Coastal Cordillera (CC: Fig. 1), amphibolitic gneisses and amphibolites were deformed by ductile transpressional shear zones that were active during or post-emplacement of gneiss igneous protoliths at ~200–191 Ma, and which are cross-cut by granite emplaced at ~174 Ma (Scheuber & Gonzalez 1999). Across South America, multiphase reactivation of pre-existing basement fault systems, such as the Gastre fault system (GF: Fig. 1) (Rapela *et al.* 1992), occurred during plate reorganization in Triassic–Jurassic times (Jacques 2003a, b).

Central and North America

In the central Oaxaca terrane of Mexico (OT: Fig. 1), post-early Permian and pre-Middle Jurassic thrusting and folding affected sedimentary rocks (Centeno-Garcia & Keppie 1999), and post Norian and pre-Aalenian (203–175 Ma) thrusting affected

Late Triassic submarine fan deposits at the contact between the Guerrero and Sierra Madre terranes in the Mesa Central of Mexico (MC: Fig. 1) (Silva-Romo *et al.* 2000). An episode of Late Triassic deformation is widespread in western Nevada (Thomson & Herve 2002). For example, Permo-Triassic marine clastic rocks of the Diablo and Candelaria formations of western Nevada (WN: Fig. 1) were overthrust by ophiolitic melange prior to emplacement of rhyolitic and dacitic dykes dated at 222–192 Ma (Thomson *et al.* 1995). Deformation fabrics associated with the Luning–Fencemaker Thrust Belt of north-central Nevada (NN: Fig. 1) formed between 201 Ma and 193 Ma with deformation probably continuing to early Toarcian (Wyld *et al.* 2001). The Cache Creek Terrane of the Canadian Cordillera (CT: Fig. 1) was imbricated by collision with the Quesnel terrane following eruption of basaltic lavas at ~210 Ma and prior to granodiorite emplacement at ~173 Ma (Harris *et al.* 2003; Lapierre *et al.* 2003). The Quesnel terrane in southeastern British Columbia (QT: Fig. 1) preserves evidence of this deformation where ~215 Ma Late Triassic diorite is deformed prior to intrusion by undeformed 197–181 Ma diorite and unconformable deposition of Early Jurassic sediments (Acton *et al.* 2002). In the Yukon-Tanana terrane of east-Central Alaska (YT: Fig. 1) Late Triassic to Early Jurassic (212 to 188–185 Ma) northwest-directed, apparently margin-parallel contraction and imbrication resulted juxtaposed deformed arc and subduction complex rocks with parautochthonous continental rocks (Hansen & Dusel-Bacon 1998). Yukon-Tanana terrane deformation of this episode in the Teslin tectonic zone of southern Yukon Territory (TZ: Fig. 1) is Late Triassic to Early Jurassic in age (Stevens & Erdmer 1996). In the McHugh Complex subduction melange of southeast Alaska (MH: Fig. 1), blueschists record a pulse of accretion at ~195 Ma (Kusky & Bradley 1999).

Eurasia

In the Late Triassic and Early Jurassic the southern Eurasian margin was affected by a major orogenic event, the Indosinian (Golonka 2004). At this time several microplates were sutured to the Eurasian margin, closing the Paleotethys Ocean (Golonka 2004). Late Triassic strike-slip and folding affected rocks from the Taimyr Peninsula in northern Russia (TA: Fig. 1) (Inger *et al.* 1999) and extends to Novaya Zemlya (NO: Fig. 1) and the south Barents Sea (Torsvik & Andersen 2002). Late Triassic deformation of sediments in the Gobi Basin of Mongolia (GB: Fig. 1) is constrained by radiometric dating to have occurred between 209 Ma and 206 Ma (Johnson 2004). Many sedimentary basins in central Asia record Late Triassic deformation (Otto 1997). Ductile shear zones in Liaoning, North China (LP: Fig. 1) show top to the southeast oblique thrusting dated at ~219 Ma by the Ar–Ar method (Zhang *et al.* 2002). Chen *et al.* (2003) described seven Mesozoic compressional phases in an overall tensional, probably subduction-related regime from southeast China, the earliest of which is Late Triassic in age and coincided with the climax of collision between the North and South China blocks (NS: Fig. 1) (Chang 1996). A syn-kinematic granite pluton, dated at ~197 Ma by the U-Pb zircon and Rb-Sr methods, times late-stage Indosinian deformation on the Songpan-Ganzi fold belt, Sichuan, west-central China (SG: Fig. 1) (Roger *et al.* 2004). Deposition in the flexural foredeep to this fold belt, the Longmen Shan foreland basin (LS: Fig. 1), spanned the time period from 227 Ma to 206 Ma (Yong *et al.* 2003). High greenschist to amphibolite grade metamorphism occurred during Late Triassic–Middle Jurassic terrane collision in the Fujian Province of southeast China (FP: Fig. 1) (Lu *et al.* 1994); similar aged collision on the Mianlue suture zone, part of the collision zone

between the North China and South China blocks, in central China is associated with major gold mineralization (NS: Fig. 1) (Vielreicher *et al.* 2003). Late Triassic–Early Jurassic deformation is also weakly developed in Peninsular Malaysia, related to collision of an amalgamated Sibumasu/Indochina/South China with North China along the Qinling–Dabei Suture Zone (Meng & Zhang 2000) and to closure of Permo-Triassic rift basins along the Song Da zone in Laos and Vietnam (SD: Fig. 1) (Metcalf 2000). The Mazar accretionary prism in the Kunlun Mountains of southwest China (KM: Fig. 1) records Late Triassic–Early Jurassic docking between the Gondwanian Karakoram-Qiangtang block and the Eurasian Kunlun block immediately prior to or during emplacement of 215–190 Ma arc plutons (Xiao *et al.* 2002). In the Karakorum, Carnian–Norian carbonate sediments folded by Eo-Cimmerian deformation of Late Triassic age are unconformably overlain by Pliensbachian–Toarcian red bed deposits (Gaetani 1997). Zircon fission track cooling ages from the northern edge of the Tibetan Plateau indicate uplift related to collision of the Qiantang block and Kunlun blocks (KM: Fig. 1) in the period 220–200 Ma, and this is reflected by a corresponding period of non-deposition or erosion in the nearby Tarim basin (Jolivet *et al.* 2001). Between the Caspian Sea and the Tien Shan in Central Asia, accretion of central Iran to the southern margin of Eurasia resulted in an intense, Late Triassic episode of deformation with development of a widespread unconformity (Thomas *et al.* 1999). The eastern part of the Donbas foldbelt of the Ukraine (DF: Fig. 1) records intense Late Triassic-aged (Cimmerian) deformation with widespread unconformity development between Triassic and Jurassic sediments (Stovba & Stephenson 1999). Blueschists in metabasite rocks along the Izmir–Ankara suture in northern Turkey (IA: Fig. 1) record a late Triassic pulse of Palaeo-Tethys subduction from 215 Ma to 205 Ma during the Cimmeride orogeny (Okay *et*

al. 2002). Cimmeride deformation in Turkey was complete by Sinemurian times (~197 Ma) (Okay *et al.* 2002).

New Zealand

Bradshaw *et al.* (1981) described a Late Triassic deformation episode, the Rangitata I orogeny, which marked the accretion of the older Rakaia sub-terrane of the Torlesse Terrane to a trench-slope basin suite represented by the Caples Terrane. White mica samples from deep levels of the Otago and Marlborough schists of South Island, New Zealand (NZ: Fig. 1), yielded Ar–Ar method ages that give a peak age for Otago Schist metamorphism of 180–170 Ma (Little *et al.* 1999). This deformation is interpreted to have resulted from collision between the Torlesse Terrane and Caples Terrane (Mortimer 1993), and corresponds in time to the Rangitata I orogeny (Bradshaw *et al.* 1981). Rb–Sr method isochron ages of Brook Street, Dun Mountain-Maitai, and Murihiku Terrane metasediments of South Island show cooling age patterns that indicate low-grade metamorphism in latest Triassic and earliest Jurassic times (Adams *et al.* 2002). This is possibly coincident with conglomerate deposition from 200–180 Ma that recorded docking between the Median Tectonic Zone and Brook Street terranes (Tulloch *et al.* 1999). Torlesse Terrane metasediments also show Late Triassic to earliest Jurassic ages (225–200 Ma) of burial metamorphism for the Rakaia Subterrane, with postmetamorphic uplift and cooling continuing through to Middle Jurassic times (~170 Ma) (Adams & Graham 1996).

Other Late Triassic–Early Jurassic events

Magmatism

Eruption of continental flood magmatism provinces (areas of lava in excess of 100,000 km²) and the formation of large igneous provinces (LIP) is characteristic of the Late Triassic–Early Cretaceous period. Three continental LIPs, two basaltic and one rhyolitic, were erupted in the period ~205–160 Ma (Marzoli *et al.* 1999; Riley & Knight 2001; Riley *et al.* 2001) with conspicuous peaks of magmatism at 200 Ma and 183 Ma. The Central Atlantic Magmatic Province (*CAMP*; Fig. 1) is one of the largest continental igneous provinces erupted during the Phanerozoic (Tanner *et al.* 2004). The province erupted largely from ~205 Ma to 199 Ma (Marzoli *et al.* 1999; Nomade *et al.* 2002) with early olivine dolerites at ~209 Ma in the Nova Scotia region (Pe-Piper & Reynolds 2000). The Gondwana Large Igneous Province (*GLIP*; Fig. 1) (Riley *et al.* 2001; Storey & Kyle 1997) includes southern African Karoo basalts, Antarctic Ferrar gabbro and Kirkpatrick basalts, and the silicic magmatic province of South America and the Antarctic Peninsula, which constitutes one of the largest silicic provinces on Earth (Pankhurst *et al.* 2000). Basaltic eruption appears to have been concentrated in a brief period at around 183–182 Ma (Riley & Knight 2001; Riley *et al.* 2004), with rhyolitic magmatism in three pulses over a more extended period between 188 Ma and 153 Ma (Pankhurst *et al.* 2000). Extensive bimodal basalt–rhyolite magmatism in the period 186–170 Ma, hosting economically important precious and base-metal mineral deposits, is also recorded from British Columbia (Evenchick & McNicoll 2002; MacDonald *et al.* 1996). Absence of an oceanic record for this period makes identification of submarine flood magmatic provinces difficult; however, at least three potential oceanic plateau candidates exist: 1) the extensive Wrangellia Terrane of northwest North America may represent an accreted basaltic

oceanic plateau that erupted at ~227 Ma (Kerr *et al.* 2000); 2) the Cache Creek Terrane of the Canadian Cordillera may represent an accreted oceanic plateau that erupted at ~210 Ma (*CTP*: Fig. 1) (Lapierre *et al.* 2003), and 3) an allochthonous tectonic unit of mafic volcanic rocks, the Nilüfer Unit of northwest Turkey, may represent a Palaeo-Tethyan, Triassic oceanic plateau accreted to the Laurasian margin during the Late Triassic (*NUP*: Fig. 1) (Okay *et al.* 2002). In addition to extrusive magmatism, major plutonic complexes of Late Triassic to Middle Jurassic age are common on the Pacific and Tethyan margins of Pangaea. For example, in the Antarctic Peninsula, plutonism was active in the Late Triassic–earliest Jurassic (220–200 Ma) (Millar *et al.* 2002; Wever *et al.* 1995), and in the Middle Jurassic (170–160 Ma) (Pankhurst *et al.* 2000). Within-plate granites of this age are also recorded from the Ellsworth–Whitmore Mountains elsewhere in West Antarctica (Storey *et al.* 1988). Plutonism in southeastern Peru, was active in the intervals 225–190 Ma and 180–170 Ma (Clark *et al.* 1990) and in Ecuador from 227 Ma to 200 Ma (Noble *et al.* 1997). Igneous rocks of Late Triassic to Early Jurassic age (228–175 Ma) are widespread in the western Cordillera of North America, and have potassic or shoshonitic compositions unlike igneous rocks before or after (Mortimer 1986, 1987). For example, in the east-central Sierra Nevada of California an intense pulse of K-rich plutonism has been identified at 180–165 Ma (Coleman *et al.* 2003) and in northwest Nevada high-K calc-alkaline plutons intruded between ~196 Ma and ~190 Ma (Quinn *et al.* 1997). In Sichuan Province, west-central China, plutonism was active from ~197 Ma to 153 Ma, in northwestern China plutonism at ~198 Ma is associated with gold mineralization (Qi *et al.* 2004), and in southeast China, Jurassic plutons intruded in the interval 175–160 Ma and cover an area of 900 x 400 km (Li *et al.* 2003). Late Triassic–Early Jurassic plutonism in the range 211–183 Ma is also recorded from the

Korean Peninsula and Japan (Arakawa *et al.* 2000; Cluzel *et al.* 1991; Kamei *et al.* 2000). Late Triassic magmatism (~220 Ma) is also evident in New Guinea (Crowhurst *et al.* 2004). In North America, peaks of kimberlite magmatism occur at ~196 Ma and 180–176 Ma (Heaman & Kjarsgaard 2000), and at ~172 Ma (Kopylova *et al.* 1998), the Yakutian kimberlite field of Siberia shows peaks in emplacement from 220 Ma to 240 Ma and from 170 Ma to 150 Ma (Heaman *et al.* 2003), in Africa a pulse of kimberlite emplacement is recognised from 190 Ma to 150 Ma (Heaman *et al.* 2003), and in Australia in the Northern Territories kimberlites are recorded at ~179 Ma (Belousova *et al.* 2001) and in South Eastern Australia at ~170 Ma (with lamproite magmatism at ~187 Ma) (Foden *et al.* 2002).

Geomagnetic field

Geomagnetic field changes around the Triassic–Jurassic boundary are small, and periods of extended polarity short, compared with what is recorded for the mid-Cretaceous period (e.g., Gallet & Hulot 1997). The Early Jurassic is relatively poorly known (Yang *et al.* 1996); however, a several million year period of anomalously low reversal rate has been observed for the Triassic–Jurassic boundary (Gradstein *et al.* 2004; Johnson *et al.* 1995). Although possibly not significant for changes at the core–mantle boundary, this is roughly an order of magnitude longer than polarity intervals during the preceding period of high reversal rate (mean ~500 ky) in the Late Triassic (Kent & Olsen 1999).

Atmosphere and oceans

Short-lived periods of extreme oceanic anoxia are recorded for the Late Triassic–Early Jurassic interval (Hesselbo *et al.* 2000) with anomalous activity extending up to the early Middle Jurassic (Hesselbo *et al.* 2003). For example, the global Early Toarcian (Early Jurassic) oceanic anoxic event (OAE) occurred at ~183 Ma (Hesselbo *et al.* 2000), and carbon isotope excursions occurred at the Triassic–Jurassic boundary (Hesselbo *et al.* 2002). Other OAEs also occurred at the end of the Norian (late Triassic; ~204 Ma) (Sephton *et al.* 2002) and in the Pliensbachian (Early Jurassic; 189–183 Ma) (Borrego *et al.* 1996). CO₂ levels, and probably atmospheric temperatures, were substantially elevated across the Triassic–Jurassic boundary (Beerling & Berner 2002), across the Pliensbachian–Toarcian boundary (Hesselbo *et al.* 2000) and in the early Middle Jurassic (174–170 Ma) (Hesselbo *et al.* 2003). Examination of carbon isotopes in wood from this time suggest huge influxes of isotopically light carbon into the upper oceans, biosphere and atmosphere, for which rapid release of methane hydrate from marine continental margin sediments has been implicated (Hesselbo *et al.* 2000; Hesselbo *et al.* 2003; Hesselbo *et al.* 2002). Indicating the scale of this event, a major enrichment is seen in $\delta^{13}\text{C}$ of hydrocarbons in the Late Triassic to Early Jurassic, one of only three such shifts seen in the Late Proterozoic and Phanerozoic (Andrusevich *et al.* 1998). Episodes of anoxia and accumulation of carbon-rich sediments resulted in formation of abundant oil source rocks, including Late Triassic–Middle Jurassic coal in Siberia (Il'ina & Shurygin 2000; Kirichkova *et al.* 2003; Kirichkova & Kulikova 2002; Kirichkova & Travina 2000). The early Toarcian was a period of sea-level rise and marine transgression (Schouten *et al.* 2000) and the Triassic–Jurassic boundary has also recently been recognized as a time of sea-level rise (Hesselbo *et al.* 2004).

Biotic changes

Two major mass extinction events occurred in the Late Triassic–Early Jurassic period. The largest, one of the "Big Five" Phanerozoic mass extinctions (Hallam & Wignall 1999; Jablonski & Chaloner 1994; Newell 1967), occurred at the Triassic–Jurassic boundary (~200 Ma) (Tanner *et al.* 2004), and the second across the Pliensbachian–Toarcian boundary (~183 Ma) (Aberhan & Fursich 2000) possibly in an extended period of extinctions lasting approximately seven million years (Little & Benton 1995). Eruption of large igneous provinces and extinction events have been causally linked but the relationships are not straightforward (Wignall 2001). Oceanic anoxia and extinction at the Pliensbachian–Toarcian boundary has been linked with eruption of the main phase of the Gondwana large igneous province (Palfy & Smith 2000; Riley & Knight 2001; Riley *et al.* 2004) and the end-Triassic extinction event has been linked with the eruption of Central Atlantic Magmatic Province (Guex *et al.* 2004; Wignall 2001). Other extinctions are recognized in this period, including one in Late Norian times affecting Monotid bivalves and most ammonoids (~204 Ma) (Sephton *et al.* 2002) and two affecting ammonites in the Early Toarcian (~180 Ma) (Cecca & Macchioni 2004).

Distribution of mid-Cretaceous deformation around the palaeo-Pacific ocean

Antarctic Peninsula

Mid-Cretaceous deformation affects rocks forming all three tectonostratigraphic terranes identified by Vaughan & Storey (2000) (AP: Fig. 2). In the Western Domain

terrane (Vaughan & Storey 2000), the Fossil Bluff Group (Butterworth *et al.* 1988; Crame & Howlett 1988; Macdonald & Butterworth 1990) is interpreted to be an Early Jurassic to late Early Cretaceous fore-arc basin sequence (Doubleday & Storey 1998; Nichols & Cantrill 2002) overlying accretionary complex rocks on Alexander Island. Deposition of sediments in this basin terminated in the late Albian (~100 Ma) with shoaling and uplift (Doubleday *et al.* 1993; Nichols & Cantrill 2002; Storey *et al.* 1996) during dextral transpression (Doubleday & Storey 1998). In the Central Domain terrane (Vaughan & Storey 2000) in northwest Palmer Land, a major flower structure, forming a sinistral transpressional transfer zone, deforms Cretaceous gabbro, Late Triassic granodiorite and marble tectonic breccia of unknown age (Vaughan *et al.* 1999). Biotite cooling ages in deformed gabbro and mafic dykes from the flower structure date sinistral shear and thrusting there at ~110 Ma (Vaughan *et al.* 1999). Mid-Cretaceous deformation is most strongly developed in the Eastern Domain terrane (Vaughan & Storey 2000). The Eastern Palmer Land Shear Zone (Vaughan & Storey 2000) is a major ductile shear zone, up to 15 km wide, formed by dextral transpression and east-directed orthogonal compression, with activity dated at ~103 Ma (Vaughan *et al.* 2002a). This biotite cooling age, dated by the Ar–Ar method, was obtained from ductilely thrust mid-Jurassic gabbro. This confirmed earlier work from eastern Palmer Land (Meneilly 1983, 1988) that suggested that east-directed overthrusts cut granodiorite dated at ~113 Ma. In the Eastern Domain farther south, in Ellsworth Land, Middle Jurassic to Early Cretaceous (Laudon & Fanning 2003) marine sediments of the Latady Formation (Laudon *et al.* 1983) are thrust and openly folded (Vaughan *et al.* 2002b). The peak of deformation coincided with emplacement of a granitoid dyke dated by the U–Pb SHRIMP method at ~107 Ma (Vaughan *et al.* 2002b). Sedimentary sequences of the Eastern Domain also show

a paucity of sediments between late Berriasian and Barremian times (Hathway 2000), prior to deposition of an Aptian to Eocene megasequence. This hiatus probably resulted from changes in deposition and erosion caused by mid-Cretaceous deformation. The continuation into the northern Antarctic Peninsula of the terranes identified by Vaughan & Storey (2000) in Palmer Land and Ellsworth Land is not clear, and evidence for mid-Cretaceous deformation is more sparse; however, this may be a function of more recent and more intense mapping activity in the southern Antarctic Peninsula. In northern Graham Land, west-directed, ocean-vergent folding and thrusting deformed mid-Cretaceous basaltic lavas of the Antarctic Peninsula Volcanic Group, dated at ~117 Ma, and these structures were cut by granodiorite plutons dated at 96 Ma (Birkenmajer 1994). In northeast Graham Land, on the margin of the Larsen Basin, localized folds and faults formed during a mid-Cretaceous episode of sinistral transpression (Del Valle & Miller 2001). East of northern Graham Land, on James Ross Island, coarse conglomerate units were deposited and rafts of extrabasinal Jurassic strata incorporated in mostly mudstone Aptian to Albian back arc sediments of the Larsen Basin (Ineson 1985, 1989; Riding & Crame 2002). Although this constitutes less direct evidence for deformation, these higher-energy events suggest that the arc was uplifted and rejuvenated in the mid-Cretaceous. At the northern tip of the Antarctic Peninsula, along the South America–Antarctica plate boundary in the vicinity of Elephant Island, Grunow *et al.* (1992) (EI: Fig. 2) interpreted that mid-Cretaceous transpression had overprinted earlier evidence for subduction activity and Trouw *et al.* (2000) placed this deformation at 110–90 Ma. East of the Antarctic Peninsula, in the Weddell Sea, Geosat radar altimetry data reveal major changes in spreading during the Cretaceous normal polarity interval (Livermore & Woollett 1993).

Other areas of Antarctica

In this volume, Siddoway *et al.* (in press) described new dyke data from Marie Byrd Land that indicate an episode of dextral shear predated formation of extensional gneiss domes in the period 105–94 Ma and prior to the onset of New Zealand–Antarctica rifting. Kinematic data from farther east along the margin (Vaughan & Storey 2000) and interpretation of seafloor data (Sutherland & Hollis 2001) support mid-Cretaceous dextral shear along this segment of the Gondwana margin. In East Antarctica, adjacent to the Rennick graben in the Lanterman Range of Victoria Land, Permo-Triassic Beacon Group sediments and Jurassic volcanic rocks are thrust and tightly folded (Roland & Tessensohn 1987), during an episode of sinistral transpression of possible mid-Cretaceous age (Tessensohn 1994) (LR: Fig. 2), although later authors have argued for Cenozoic-aged deformation (Rossetti *et al.* 2003).

South America

Dalziel (1986) noted the synchronicity of the first phase of mid-Cretaceous deformation (Mirano diastrophic phase, 112–105 Ma; MD: Fig. 2) along the western margin of South America from the Magellan Basin to the West Peruvian Trough, post-dating Aptian-Albian sediments and predating intrusions and sediments formed from 105–80 Ma. Evidence of hiatuses in sedimentation is also widespread in western South America in mid-Aptian and Aptian–Albian times (Macellari 1988). An unconformity related to one of these hiatuses cuts felsic tuff, dated at ~104 Ma, in the

Andes of central Chile (Charrier *et al.* 1996). Thrusting deformed Aptian–Albian sedimentary and ophiolitic rocks of the mid-Jurassic to Lower Cretaceous Rocas Verdes basin in South Georgia (SG: Fig. 2) (Macdonald *et al.* 1987) and in southern Patagonia (Dalziel 1986) and is linked to closure of a back-arc basin with associated ophiolite obduction (Dalziel 1981). In Cordillera Darwin (Kohn *et al.* 1993) (CD: Fig. 2) amphibolite facies metamorphism of Palaeozoic basement rocks is associated with thrust-related deformation of upper Aptian–Albian sedimentary rocks (Dott *et al.* 1977) with shortening of over 430 km from 110 Ma to 90 Ma (Halpern & Rex 1972) in the mid-Cretaceous (Kraemer 2003). Cunningham (1995) pointed out that this orogeny exhumes some of the highest metamorphic grade rocks in the Andes south of Peru and demonstrated a transpressional component to deformation with strain partitioning.

In northern Chile, the Atacama fault system (AF: Fig. 2) exhibits transpressional movement and uplift which deformed plutonic and volcanic rocks older than ~111 Ma (Thiele & Pincheira 1987) and arc activity ceased in the mid-Cretaceous in that area (Brown *et al.* 1993). The fault system was inverted in post-Early Cretaceous times by contractional deformation that also resulted in widespread thin-skin thrust deformation of sediments (Grocott & Taylor 2002). Late Albian compression folded Lower Cretaceous submarine volcanic sequences in western Peru (Mochica deformation event of Mégard 1984) (ME: Fig. 2). Late Albian uplift and erosion of mid-Albian sandstones is evident in western Columbia (Barrio & Coffield 1992) (WC: Fig. 2), and late Early Cretaceous metamorphism and deformation of Upper Jurassic to Lower Cretaceous arc rocks is widespread from Columbia to Mexico (Dickinson & Lawton 2001; Tardy *et al.* 1994). White mica and amphibole Ar–Ar

method ages from high pressure metamorphic rocks in the Coastal Fringe/Margarita belt of northern Venezuela (part of the Caribbean–South American plate boundary, NV: Fig. 2) suggest that transpressional deformation occurred in mid-Cretaceous times at ~96 Ma (Smith *et al.* 1999).

Central America and Caribbean

In Hispaniola, Puerto Rico and the Virgin Islands (HI: Fig. 2), Lower Cretaceous island-arc rocks, believed to have formed part of a southwest-facing arc in the Early Cretaceous (Pindell & Barrett 1990), are truncated by a major erosional unconformity overlain by shallow-water, Aptian-Albian limestone (Lebron & Perfit 1993). Draper *et al.* (1996) linked this to thrust emplacement of the Hispaniola peridotite belt in Aptian–Albian times. In Cuba, the Antilles arc accreted basaltic rocks of ocean plateau affinity in the period 112–91 Ma (Kerr *et al.* 1999).

Phengitic micas from the southern belt of the Motagua fault zone of Guatemala (GU: Fig. 2) yield Ar–Ar method deformation ages in the range 125–113 Ma, recording mid-Cretaceous collision of the Chortis Block with western Mexico (Harlow *et al.* 2004). Early to mid-Cretaceous uplift and erosion affects a Barremian to mid-Albian limestone sequence in Honduras (Weiland *et al.* 1992) (HO: Fig. 2). Dickinson & Lawton (2001) described the accretion of an arc terrane to the Mexican margin in late Early Cretaceous time. In Mexico, greenschist facies metamorphism, linked to collision of the Guerrero terrane (Tardy *et al.* 1994) (GT: Fig. 2) affects plutons dated to be between 112 and 101 Ma (Stein *et al.* 1994).

North America

In southern California, ocean-vergent, southwest-directed overthrusting has deformed 118 Ma, magmatic-arc granodiorite of the western Peninsular Ranges batholith (PR: Fig. 2) with the formation of mylonite zones dated at 115 Ma (Thomson & Girty 1994). Mylonite and granodiorite are truncated by 105 Ma tonalite (Thomson & Girty 1994) and deformation was probably active in the period 115–108 Ma (Johnson *et al.* 1999). West-directed (i.e. oceanward) compression of the western Peninsular Ranges batholith in southern and Baja California also predated onset of emplacement of the eastern Peninsula Ranges batholith at 99 Ma (Kimbrough *et al.* 2001). A peak of Franciscan melange blueschist metamorphism appears to have occurred at this time (Ernst 1993). In the Sierra Nevada of California (SN: Fig. 2) a major episode of thrusting is recognized deforming Jurassic and Cretaceous plutonic rocks between ~110 Ma and ~92 Ma (Mahan *et al.* 2003). For example, contractional deformation on the Bench Canyon shear zone shows multiple phases from ~101 Ma with a peak at ~95 Ma (McNulty 1995), and synkinematic sheared orthogneiss from the Tiefort Mountains is dated at ~105 Ma (Schermer *et al.* 2001). A major thrust system of mid-Cretaceous age is developed along much of the Coast Belt of northwestern North America (CB: Fig. 2) (Umhoefer & Miller 1996). Regional mid-Cretaceous deformation is recognized in British Columbia (MacDonald *et al.* 1996) (BC: Fig. 2), with, for example, ocean-vergent thrusting (Journey & Friedman 1993) of upper Valanginian to middle Albian volcanic rocks. Thrusting was active from at least mid-Albian times to the emplacement of synkinematic plutons dated at ~97 Ma and ~96 Ma and deformed an accretionary complex that formed prior to 92 Ma (Chardon 2003). In Cretaceous sedimentary sequences of northwestern Canada,

major, regionally extensive unconformities exist in mid-Aptian, and between Albian and Cenomanian, strata (Dixon 1993, 1997). On Duke Island, in southeast Alaska, a major and widespread episode of thrusting deformed ultramafic and arc rocks intruded from 111 Ma to 108 Ma (Butler *et al.* 2001) (DI: Fig. 1). In central and northern Alaska, ductile, north-directed overthrusting was active with blueschist and amphibolite-facies metamorphism dated at ~108 Ma. This formed during an episode of overall extension and metamorphic core-complex formation in the southern Brooks Range (Till *et al.* 1993; Till & Snee 1995) and major thrusting and tectonic transportation of ophiolite terranes was coeval in the northern Brooks Range (Cole *et al.* 1997).

East and Southeast Asia

In the Anadyr-Koryak region of northeast Russia (AK: Fig. 2), Albian to Cenomanian volcanic rocks, and Barremian-Aptian and Albian clastic sequences, unconformably overlie folded Callovian to Hauterivian island-arc rocks and Palaeozoic to Hauterivian arc marginal volcano-sedimentary sequences (Filatova & Vishnevskaya 1997; Stavsky *et al.* 1990). Deformation occurred in Barremian–Aptian (~120 Ma) and Albian (~105 Ma) times (Filatova & Vishnevskaya 1997; Stavsky *et al.* 1990). In the Chukotka Peninsula of the Anadyr-Koryak region, compressional deformation from 124 Ma to 117 Ma, based on Ar–Ar method dating of polydeformed greenschist- grade phyllites and marbles, is followed by a period of metamorphic core complex formation from 109 Ma to 104 Ma (Toro *et al.* 2003). Ophiolitic thrusting in the Sikhote-Alin mountain range, eastern Siberia (SA: Fig. 2), is dated at ~110 Ma by the Ar–Ar method (Faure *et al.* 1995). Ophiolitic rocks in

northern Japan (NJ: Fig. 2), containing a conformable sequence of Tithonian pelagic sedimentary rocks and Hauterivian to post-Aptian terrigenous fore-arc sedimentary rocks, were underthrust and accreted with uplift and metamorphism of arc rocks from Barremian times (130–125 Ma) to at latest the time of blueschist metamorphism dated at 110 Ma (Kimura 1997; Kimura *et al.* 1994). Some evidence for a continuation of more rapid accretion is suggested by more intense metamorphism of ophiolitic units accreted between Aptian and Cenomanian times (Kiyokawa 1992; Ueda *et al.* 2000). Sanbagawa metamorphism is estimated to have occurred between ~120 and ~110 Ma, with a peak at ~116 Ma, in central Shikoku, Japan (Isozaki & Itaya 1990; Okamoto *et al.* 2004) (SH: Fig. 2). Associated metamorphism at ~116 Ma is also recorded for the Japanese Median Tectonic Line in the South Kitakami and paleo-Ryoke belts in central Japan (Sakashima *et al.* 2003) (CJ: Fig. 2). In the Fujian Province of southern China (FP, Fig. 2), gabbroic and ultramafic rocks of a dismembered ophiolite suite (Wang & Lu 1998) were emplaced on Paleozoic basement rocks by ocean-vergent thrusting coeval with ~115 Ma gabbro and granitoid plutons (Wang 2002), and compressional shear joints dated at 107 Ma (Lu *et al.* 1994). Fission track dating also suggests that uplift had ceased by ~110 Ma (Chen *et al.* 2002). Ar–Ar method cooling ages from the Changle-Nanao ductile shear zone in the same region suggest rapid uplift during the period 118–107 Ma (Wang & Lu 1997). In the Qilian Shan of western China (QS: Fig. 1), apatite and zircon fission track ages indicate a multiple-phase history of exhumation in the period 115–90 Ma (George *et al.* 2001) and the Bainang terrane in the Yarlung-Tsangpo suture of southern Tibet records post-late Aptian accretion of Tethyan oceanic rocks (Ziabrev *et al.* 2004). Farther west in the Karakoram, Tethyan margin, shallow marine sediments of Aalenian to Lower Cretaceous age and crystalline basement rocks are incorporated in huge thrust sheets

that are capped by thick deposits of mid-Cretaceous conglomerate (Gaetani 1997). The Truong-Son belt, of north-central Vietnam (TS: Fig. 2), shows metamorphism and mylonite formation in the period 120–90 Ma with notable peaks at ~115 Ma and between 106 Ma and 103 Ma (Lepvrier *et al.* 1997). In the western Philippines (WP: Fig. 2), east-directed thrusting deforms Lower Cretaceous ophiolitic rocks unconformably overlain by a middle Eocene hemipelagic sedimentary sequence (Faure *et al.* 1989), which is possibly related to the collision of the West Philippine block with the China-Indochina margin in latest Early Cretaceous times (Lapierre *et al.* 1997). In Java, Sulawesi, and Kalimantan (JS: Fig. 2), an extensive high pressure-ultra-high pressure metamorphic basement terrane was recrystallized and uplifted during collision of a Gondwanan continental fragment with the Sundaland margin between 120 Ma and 115 Ma (Parkinson *et al.* 1998).

Australia

In the Surat basin of eastern Australia (SB: Fig. 2), uplifted and eroded upper Aptian marine sedimentary rocks are unconformably overlain by early Albian, paralic sedimentary rocks (Harrington & Korsch 1985; O'Sullivan *et al.* 2000). This is event also affected basins in northeastern Australia (Laura and Carpentaria) (CA: Fig. 2) and Papua New Guinea (Papuan) (PB: Fig. 1) (Haig & Lynch 1993). It is associated with increased Aptian–Albian tectonism in the eastern half of Australia, supported by fission track evidence for increased exhumation rates (Marshallsea *et al.* 2000) and palaeobathymetric evidence for non-eustatic changes in base level (Campbell & Haig 1999; Henderson 1998). In the New England orogeny of eastern Australia, mid-Cretaceous deformation (WI: Fig. 2) affected voluminous ($1.4 \times 10^6 \text{ km}^3$) volcanic

and plutonic rocks of the Whitsunday Volcanic Province and others (WVP: Fig. 2) dated at between 132 Ma and 95 Ma (Bryan *et al.* 2000; Harrington & Korsch 1985), although the age of deformation may be more tightly constrained because magmatism peaked between 120 Ma and 95 Ma (Bryan *et al.* 1997). Deformation is largely expressed as open folds associated with major faults (O'Sullivan *et al.* 2000), and may be associated with a major phase of extension in eastern and southeastern Australia in the middle Cretaceous (O'Sullivan *et al.* 1996; O'Sullivan *et al.* 2000).

New Zealand

The tectonic situation of New Zealand is complex, with a terrane interpretation that has evolved rapidly (e.g., Kear & Mortimer 2003; Leverenz & Ballance 2001; Mortimer 2004) since early suggestions for South Island (Coombs *et al.* 1976) and North Island (Sporli 1978) and comprehensive definition by Bradshaw (1989). Deformation of Early Cretaceous age was first recognized in New Zealand (the Rangitata II phase of Bradshaw *et al.* 1981), where it was initially interpreted as a phase of deformation affecting convergent margin terranes. The age of deformation is based on widespread Aptian, Albian, and intra-Albian angular unconformities in sedimentary rocks of eastern New Zealand (Bradshaw 1989), with a mid- to late Albian age of last deformation (~105 Ma, Bradshaw 1989; ~100 Ma, Laird & Bradshaw 2004). Since the key papers by Bradshaw *et al.* (1981) and Bradshaw (1989), much evidence has come to light for different aged metamorphic events in different parts of New Zealand, for example, at ~116–105 Ma in Fiordland (Klepeis *et al.* 2004), 100–85 Ma in the Wellington region (Adams & Graham 1996; Kamp 2000), 86 Ma in the Southern Alps (Vry *et al.* 2004) and 71 Ma in Otago (Mortimer &

Cooper 2004). In addition, an episode of rifting has been identified associated with local high temperature extension and magmatism, which formed the Paparoa metamorphic core complex between 110 and 90 Ma (Muir *et al.* 1997; Spell *et al.* 2000). Metamorphic events in the Southern Alps and Otago at ~86 Ma and ~71 Ma are probably related to final collision of the Hikurangi Plateau and the opening of the Tasman Sea (Mortimer & Cooper 2004; Vry *et al.* 2004). These post-date contractional deformation being considered here. The older events, from Fiordland and the Wellington region, fall in the range of mid-Cretaceous deformation from other parts of the Pacific basin margin. In the Fiordland region of southern South Island, contractional deformation was coeval with magma emplacement of the Median Batholith from 116 Ma to 105 Ma (Klepeis *et al.* 2004) (SI Fig. 2). Mid-Cretaceous compression overlaps in age with formation of the hyper-extensional Paparoa metamorphic core complex which was magmatically active from 110 Ma to 90 Ma (Muir *et al.* 1997); however, the earliest depositional ages from intercalated tuffs suggest that the switch from compression to extension was at ~101–102 Ma (Bradshaw *et al.* 1996; Muir *et al.* 1997) and oroclinal bending associated with mid-Cretaceous compression had probably ended by 110 Ma (Bradshaw *et al.* 1996). In southern North Island (NI Fig. 2), low temperature metamorphism of sandstones of the accretionary Pahau Subdivision of the Torlesse Terrane (Adams & Graham 1996), and deformation, is dated by zircon fission track data to have occurred in the period 100–85 Ma (Kamp 2000). Deformation is represented, for example, by folded, Upper Jurassic to Aptian-Albian argillic and metabasic rocks in the Wellington region, interpreted to be part of a dismembered seamount (George 1993), which are cut by ~99 Ma lamprophyre dikes.

New Zealand and expression of plate boundary forces

New Zealand is one of the best-studied areas, which has revealed that mid-Cretaceous deformation there has a complex expression. An examination of Cenozoic to Recent tectonic activity in New Zealand illustrates the kind of variation that can be seen along quite short stretches of an active margin. In particular, superimposed on the pre-rift (Laird & Bradshaw 2004) terrane complexity described by Bradshaw (1989) and Mortimer (2004) is the large-scale, ~460 km (Sutherland *et al.* 2000), Cenozoic movement of the Alpine Fault (Norris *et al.* 1990). The fault is a distributed strike-slip transfer zone (Hall *et al.* 2004) between east-directed subduction to the south (Norris & Cooper 2003) and west directed subduction to the north (Delteil *et al.* 2003) and illustrates that the expression of plate boundary forces is not necessarily straightforward. In this context, the plate boundary forces, changes in subduction rate, potential slab capture, and collision of the Hikurangi Plateau, all of which combined to drive mid-Cretaceous deformation in New Zealand may have been expressed in different but co-existing ways. In South Island, we probably see the most straightforward expression, where accelerated plate motion and heat flow are likely to have driven magmatism and contractional deformation in the period 116–105 Ma. In North Island, the situation was complicated by the approach of the Hikurangi Plateau (Vry *et al.* 2004) and a possible ridge–trench collision (Luyendyk 1995). Contractional deformation appears to have stopped at about 100 Ma, followed by a period of slab roll-back and extension prior to final collision of the Hikurangi Plateau at ~86 Ma. This was followed by opening of the Tasman Sea (Vry *et al.* 2004) and associated basins (Carter 1988), and onset of New Zealand–Antarctica rifting (Laird & Bradshaw 2004).

Other mid-Cretaceous events

Magmatism

Eruption of submarine basalt plateaux (areas of oceanic lithosphere with thickness > 10 km) and the formation of basaltic large igneous provinces (LIP) is characteristic of the mid-Cretaceous period (Kerr *et al.* 2000). Six oceanic LIPs were erupted in the period 122–88 Ma (Coffin & Eldholm 1994; Mortimer & Parkinson 1996) with conspicuous peaks of magmatism at 122 Ma and 90–88 Ma (Kerr *et al.* 2000). The Ontong-Java Plateau (*OJP*: Fig. 2) is the largest known in the geological record (Coffin & Eldholm 1994) and erupted in close proximity to the Manihiki (*MAP*: Fig. 20 and Hikurangi (*HIP*: Fig. 2) plateaus. Fragments of an Aptian–Albian oceanic plateau that accreted to the Antilles arc (*LAP*: Fig. 2) in the period 112–91 Ma are preserved in Cuba (Kerr *et al.* 1999). Not all plume impact sites were under oceanic lithosphere. The Rajmahal Traps of eastern India were erupted at ~ 118 Ma and were possibly related to emplacement of the chemically similar Kerguelen Plateau at the same time (Kumar *et al.* 2003) and the second phase of the Bunbury basalts of western Australia (*BUB*: Fig. 2), which erupted at ~ 123 Ma (Courtillet & Renne 2003). All three are closely spatially associated on reconstructions of Gondwana, and pre-date rifting-off of India (Kumar *et al.* 2003). New evidence suggests that the Bermuda plume was responsible for 2–3 km of mid-Cretaceous uplift with erosion and magmatism in the Mississippi Embayment (Cox & Van Arsdale 2002), and Maher (2001) has identified a largely terrestrial, mid-Cretaceous high-Arctic large igneous province, with magmatic ages currently poorly constrained in the

range 135–90 Ma. As in the case of the Bermuda plume, the high-Arctic province is associated with uplift and denudation. For example, mid-Cretaceous apatite fission track cooling ages in Carboniferous sediments, probably associated with exhumation, have been recorded in East Greenland at this time (Johnson & Gallagher 2000); a widespread mid-Cretaceous unconformity is developed in the northern part of the mid-Norwegian margin (Lundin & Dore 1997); and an associated unconformity is developed as far south as the Atlantic Western Approaches Trough (Ruffell 1995). Granitic magmatism also shows a widespread mid-Cretaceous peak. The Lassiter Coast intrusive suite of the southern Antarctic Peninsula, which covers an area of ~500 x 100 km, shows a major peak in magmatism between about 115 and 95 Ma (Pankhurst & Rowley 1991). A major peak of I-type magmatism is evident in Thurston Island with emplacement from 125 Ma to 110 Ma (Pankhurst *et al.* 1993), and a pulse of A-type granitoid magmatism is recorded in western Marie Byrd Land between 115 Ma and 95 Ma (Siddoway *et al.* in press). Bruce *et al.* (1991) identified a mid-Cretaceous peak of Andean magmatism occurring between 120 Ma and 70 Ma and the North Patagonian Batholith shows a peak of emplacement between 120 Ma and 90 Ma (Pankhurst *et al.* 1999). This is supported by palaeomagnetic data that suggests that the major part of the North Patagonian Batholith was intruded during the Cretaceous Long Normal Interval (Beck *et al.* 2000). A pulse of plutonism is seen in central Mexico from 110 Ma to 100 Ma (Stein *et al.* 1994). The 800 km-long eastern Peninsula Ranges batholith of southern and Baja California was intruded between 99 Ma and 92 Ma with interpreted magma flow rates comparable to those estimated for flood basalt eruptions (Kimbrough *et al.* 2001); the western Peninsular Ranges batholith of Baja California shows a peak of tonalite magmatism between 115 Ma and 103 Ma (Tate & Johnson 2000). In California, plutonism in the east-central Sierra

Nevada batholith is concentrated in a brief period from 102 Ma to 86 Ma (Coleman *et al.* 2003); the voluminous Tuolumne intrusive suite of the Sierra Nevada batholith was emplaced between ~95 Ma and ~85 Ma (Coleman *et al.* 2004). A newly recognized episode of cauldron subsidence with emplacement of rhyolite domes occurred from 107 Ma to 104 Ma in central British Columbia (MacIntyre & Villeneuve 2001). Tin-associated magmatism in the Khingan-Okhotsk belt of eastern Siberia, extending over 400 km, occurred episodically in a short period around ~95 Ma (Sato *et al.* 2002). The adakitic, Separation Point magmatic suite and associated orthogneisses, the Karamea batholith, and the Paparoa batholith, all of the Median Batholith of New Zealand were emplaced in the period 120–105 Ma (Mortimer *et al.* 1999; Muir *et al.* 1998; Muir *et al.* 1997; Waight *et al.* 1998). Kimberlite magmatism also peaked in the mid-Cretaceous, with a period of increased emplacement rate in Russia from 105 Ma to 95 Ma, in North America from 103 Ma to 94 Ma, and in Africa from 116 Ma to 70 Ma (with a brief hiatus from 100 Ma to 95 Ma) (Heaman *et al.* 2003).

Post-compressional extension

In general, mid-Cretaceous compression is followed by extension or transtension, usually from ~100 Ma on, and often on a spectacular scale, probably as a function of the high heat flow associated with a superplume event. In New Zealand, Marie Byrd Land, and eastern Siberia metamorphic core complexes formed (Muir *et al.* 1997; Siddoway *et al.* 2004; Siddoway *et al.* in press; Toro *et al.* 2003). Ductile extensional structures formed from 105 Ma to 94 Ma following thrusting of the Peninsular Ranges batholith in southern California (Thomson & Girty 1994),

transtensional basins formed in the Canadian Cordillera (Bassett & Kleinspehn 1996), and major extensional basins formed following widespread thrusting in Alaska (Till *et al.* 1993).

Geomagnetic field

The Cretaceous long normal polarity interval of the geomagnetic field (e.g., Gallet & Hulot 1997) lasted from 125–84 Ma and is one of the key pieces of evidence for the mid-Cretaceous superplume event (Larson 1991b). There is some disagreement over the intensity of the geomagnetic field during the Cretaceous long normal polarity interval, which some models suggest should have been stronger than normal (Tarduno *et al.* 2001). Measurements of geomagnetic field intensity are difficult to make (McElhinny & Larson 2003) and complicated by post-preservation changes (Dobrovine & Tarduno 2004). Although new evidence suggests that the geomagnetic poloidal field intensity was reduced just prior to (Pan *et al.* 2004) and during (Biggin & Thomas 2003) the Cretaceous long normal interval, other authors (Tarduno *et al.* 2001, 2002) present convincing evidence that the field was up to three times stronger than in the preceding Late Jurassic or following Cenozoic.

Atmosphere and oceans

Short-lived periods of extreme oceanic anoxia are recorded for the mid-Cretaceous interval (Handoh & Lenton 2003; Leckie *et al.* 2002). For example, the global Selli ocean anoxic event (OAE-1a) occurred between 120.5 and 119.5 Ma (Larson & Erba 1999), and the global Bonarelli OAE-2 occurred at the Cenomanian–

Turonian boundary (~93.5 Ma) (Pancost *et al.* 2004). Other events that are more restricted in distribution within Tethys occurred at 113–109 Ma (OAE-1b) and ~99.5 Ma (OAE-1d) (Leckie *et al.* 2002). Maximum sea surface temperatures were 3–5 degrees warmer than today, but with pronounced variability that possibly triggered OAEs (Wilson & Norris 2001). Reef drowning is also characteristic of this period (Wilson *et al.* 1998) and the mid-Cretaceous period saw some of the highest sea levels in the Phanerozoic (Haq *et al.* 1987) with highstands in the Early Aptian (~118 Ma), Late Albian (~102 Ma), and Turonian (93–90 Ma) (Strasser *et al.* 2001). Episodes of anoxia and accumulation of carbon-rich sediments, resulted in major accumulation of oil source rocks (e.g., Nzoussi-Mbassani *et al.* 2003), including abundant coal offshore Nigeria (e.g., Obaje & Hamza 2000), and the mid-Cretaceous is the most prolific of six periods of accumulation of effective oil source rocks during the Phanerozoic (Andrusevich *et al.* 1998).

Biotic changes

Apart from an extinction event at the Cenomanian–Turonian boundary (~94 Ma) (Harries & Little 1999), in terms of disappearance of major groups, the Cretaceous long normal polarity interval (125–84 Ma) is generally only associated with higher rates of turnover in mineralized plankton taxa (Leckie *et al.* 2002). Rather than going extinct, faunal and floral groups experienced major radiations in this period, which appears to have been the peak of the so-called "Mesozoic Marine Revolution" (Alroy 2004; Bambach 1999; Vermeij 1995). The angiosperm and pollinating insect taxa went through a major expansion at this time (Grimaldi 1999; Kress *et al.* 2001; Lupia 1999), as did several fern groups (Nagalingum *et al.* 2002). Many groups of tetrapods

radiated into their main modern groups, including frogs, turtles, lizards, snakes, and birds (Benton 1996). Among marine invertebrates, speciation was particularly marked among some groups of bryozoans (Jablonski *et al.* 1997) and a peak in bivalve diversity is also recognized (Checa & Jimenez-Jimenez 2003).

Discussion and model

In this section, some key similarities between Late Triassic–Early Jurassic and mid-Cretaceous deformation events will be outlined and a unified conceptual model for break-up of large plates will be presented.

Late Triassic–Early Jurassic deformation, Pangaea and Mesozoic oceans

Episodic periods of coincident continental rifting and marginal collision have been described for the Tethyan Ocean from Late Permian to Late Eocene times, with significant events in the mid-Late Triassic and end-Early Cretaceous (Kazmin 1991; Ricou 1994). What singles out the Late Triassic–Early Jurassic deformation is that it occurred at a time when Pangaea was starting to break-up, and when extension, rather than compression, would have been expected to dominate plate kinematics. The pre-break-up configuration of Pangaea only came into being in the Late Permian (Muttoni *et al.* 2003) and Pangaea break-up models have the added feature of needing to accommodate the presence of a partially intra-supercontinent ocean, Tethys (Fig. 1), with differently evolving margins in its eastern and western parts (Ricou 1994). The relationship between Triassic Palaeo-Tethys and the Pangaea-surrounding, Panthalassic Ocean (Fig. 2) is comparable to the relationship between the Indian and

Pacific oceans today. In terms of plate motions, apparent polar wander paths for North America show significant changes in velocity at ~200 Ma and ~160 Ma (Beck & Housen 2003), the earlier of which would have coincided with Late Triassic–Early Jurassic deformation on the Pangaea margin. Recently, it has been shown that a global pulse of ophiolite obduction events also occurred in the Late Triassic–Early Jurassic (Vaughan & Scarrow 2003) (Fig. 3), which is consistent with the widespread evidence for Pangaea-margin compression at this time. Although it is not possible to determine a cause and effect relationship with Pangaea-events, formation of the Pacific Plate, dated at 175–170 Ma (Bartolini & Larson 2001; Fisk & Kelley 2002), followed a major oceanic plate reorganization at ~190 Ma (Nakanishi *et al.* 1992). This coincided with initial break-up of Pangaea associated with increased subduction rates at its outer margins (Bartolini & Larson 2001).

Mid-Cretaceous deformation and Cretaceous oceans

Mid-Cretaceous compressional deformation is not restricted to the margins of the palaeo-Pacific basin (Fig. 2) and is extremely widely developed, even more widely so than summarized here. For example, the northern margins of Neo-Tethys in the Mediterranean region also show deformation of this age, for example in northern Spain (Monie *et al.* 1994), Corsica (Malavieille *et al.* 1998), Slovakia (Plasienska 2003), Hungary (Haas & Pero 2004), and Greece and Bulgaria (Zagorcev 1994). Although not directly associated with initiation of continental break-up, mid-Cretaceous deformation is closely followed in several areas by episodes of high rates of extension, as outlined above, and in the case of New Zealand by rifting-off and drifting of a continental fragment from Gondwana. Major reorganization of the

Pacific Plate occurred at 120 Ma (Nakanishi & Winterer 1998; Sutherland & Hollis 2001) coincident with eruption of magmas associated with the formation of the Ontong-Java plateau among others (Kerr *et al.* 2000). Apparent polar wander paths for North America show significant changes in velocity at ~125 Ma and ~88–80 Ma (Beck & Housen 2003) and the period 125–84 Ma shows ocean crust production rates that are 50% to 75 % higher than the rates before and after this period (Larson 1991b).

Superplume–lithospheric plate interaction

The following features unify Late Triassic–Early Jurassic and mid-Cretaceous deformation: 1) Both occurred at a time of elevated mantle heat flow, as evidenced by concentrated episodes of voluminous magmatism on the continents and in the oceans; 2) both appear to have occurred at times of anomalously low reversal rate of the geomagnetic field (although this is less clear for the Late Triassic–Early Jurassic event), further implicating the mantle in whatever caused them; 3) both are followed by periods of unusually high rates of continental extension, Pangaea/Gondwana break-up in the Late Triassic–Early Jurassic case and extensional core complex formation in the mid-Cretaceous case; 4) both are associated with oceanic plate reorganization and major changes in plate velocity; 5) both occurred at times of substantial environmental and biotic change. This co-occurrence of extreme global magmatic, geomagnetic, environmental and biotic events points to one particular causal mechanism, involving simultaneous ascent of multiple hot plumes of material from the deep mantle, a "superplume event" (Larson 1991b, 1992). The global distribution of hotspot magmatism, involving substantial continental and oceanic expressions in Late Triassic–Early Jurassic and mid-Cretaceous times as outlined

above, makes more local mechanisms, such as thermal blanketing (e.g., Anderson 1998) less likely to have been responsible. Figure 3 illustrates some of the events coeval with Late Triassic–Early Jurassic and mid-Cretaceous deformation and shows the distribution of proposed superplume and geomagnetic events, major tectonism, ophiolite obduction, sea-level variation, and biotic and environmental changes through the Phanerozoic.

The relationship between deformation and superplume events will be discussed in detail below; however, it is worth touching briefly on the relationship between the rise of hot plumes of mantle material to shallow levels and the magmatic and palaeoenvironmental changes outlined above. The relationship between magmatism and advection of heat to the upper mantle is the easiest to understand. As described above, flood volcanism, plutonism and kimberlite emplacement appear to be coeval in the Triassic–Jurassic and mid-Cretaceous periods. For example, the widespread distribution of A-type, I-type and adakitic plutonism around the Pacific basin in the period 125–90 Ma, coeval with oceanic LIP and kimberlite emplacement, points to elevated heat flow over a large area of the globe. The situation for palaeoenvironmental proxy data in the Late Triassic–Early Jurassic and mid-Cretaceous period and links with high rates of volcanism is less clear, and the subject of much discussion (e.g., Hesselbo *et al.* 2002; Larson & Erba 1999). Much current interest is focussed on the possibility that small, initial magmatism-related phenomena can trigger larger palaeoenvironmental changes (Beerling & Berner 2002; Tanner *et al.* 2004). The trigger mechanisms include thermally driven elevation in crustal heat flow (Jahren 2002), fall in sea-level (Paull *et al.* 1991), CO₂-driven atmospheric warming (Beerling & Berner 2002; Jenkyns *et al.* 2001), or uplift of ocean floor

(Jahren 2002). These are invoked to trigger catastrophic, massive dissociation of methane hydrate deposits in shallow marine settings (Jenkyns *et al.* 2001) or at continental high latitudes (Kidder & Worsley 2004), with consequent large rises in atmospheric temperature, changes in ocean and atmosphere composition, and biotic radiations and extinctions (Jahren 2002; Retallack 2002; Tanner *et al.* 2004).

Late Triassic–Early Jurassic and mid-Cretaceous deformation post-date the start of their respective superplume events by only a few million years, whereas ophiolite obduction pulses follow up to 10–20 million years later. Vaughan & Scarrow (2003) suggested that this delay may be a consequence of the time it takes to close a back-arc basin, the commonest setting for ophiolitic source rocks, following a change in plate boundary forces. The evidence for both episodes of deformation outlined above, and summarized in Tables 1 and 2, suggests that deformation was concentrated in a short time period, of the order of five million years. Late Triassic–Early Jurassic deformation appears to have occurred between 202 and 197 Ma and mid-Cretaceous deformation in two periods ~116–110 Ma in the west palaeo-Pacific and ~ 105–99 Ma in the east palaeo-Pacific, with both events possibly represented in northeast Siberia (Filatova & Vishnevskaya 1997; Stavsky *et al.* 1990). The geological record indicates an abrupt onset for superplume events and consequently there has been much discussion of a triggering mechanism, usually involving changes in mantle convection state and geomagnetic field behaviour following sudden transfer of ponded cold subducted material into the deep mantle (Condie 1998; Solheim & Peltier 1994; Tackley *et al.* 1994). Associated cooling at the core–mantle boundary is argued to be a possible cause of perturbations of the geomagnetic field (e.g., Muller 2002). One of the main, large-scale effects inferred for a superplume event is heating of the upper

mantle and thermal elevation of the overlying lithosphere (Larson & Kincaid 1996) and developing the model proposed by Vaughan (1995) we will argue here that this is the key process responsible for superplume-related deformation.

"Oceanic" case

Rising mantle plumes associate with the mid-Cretaceous superplume event largely impacted oceanic lithosphere. Vaughan (1995) argued that for deformation associated with the mid-Cretaceous superplume event, which we will refer to as the "oceanic" case (Fig. 4), thermal uplift and rejuvenation of ocean floor during multiple hot plume impact at the base of the lithosphere resulted in increased gravity sliding from a broad (~10,000 km across according to Larson (1991b)) topographic high which increased ridge push. Figure 4a shows the pre-superplume state with a notional large ocean with single spreading ridge and a back-arc basin floored by oceanic lithosphere. The subducting margins of the large ocean are in a state of mild tension, which is the common observed situation globally today (Hamilton 1994). In Figure 4a, this is a result of roll-back of the old and cold subducting slab at the trench. The margins of the smaller, younger back-arc basin are in mild compression because of ridge-push forces. The commonest model for the mechanism that triggers superplume events involves accumulation of cold subducted slab material at the 670 km discontinuity or phase boundary (Machetel 2003; Tackley *et al.* 1994) and this accumulation is depicted in Figure 4a. Figure 4b shows the onset and effects of a superplume event. The 670 km discontinuity is inferred to be an endothermic phase boundary, i.e. with a negative Clapeyron slope (e.g., Mambole & Fleitout 2002), in other words energy is required to cross the boundary downwards which means it acts

as a barrier to further descent of upper mantle material into the lower mantle. Models for the onset of superplume events suggest that gravitational potential energy of accumulating cold subducted material is eventually sufficient to overcome the resistance of this phase boundary (Solheim & Peltier 1994) and a mantle avalanche is generated that descends rapidly to the core–mantle boundary (Fig 4b). This has two effects on mantle convection: an initial broad return flow that elevates the 670 km discontinuity and the upper mantle, followed by deep-rooted mantle plumes generated from increased lateral thermal variation at the core–mantle boundary (Larson & Kincaid 1996). This heating and elevation of the upper mantle triggers large-scale adiabatic decompression melting and magmatism (Larson & Kincaid 1996). The advected heat to the upper mantle has the effect of uplifting and thermally rejuvenating oceanic lithosphere over a broad area and, by topographically elevating the ridge, increasing ridge push force. A larger ridge push force increases the convergence rate at subduction zones and thermal rejuvenation of oceanic lithosphere increases the degree of coupling between the subducting and overriding plate, both of which combine to produce ocean-marginal compression. In Figure 4b, this is expressed as, for example, back-arc basin closure and arc collision or ophiolite obduction (Vaughan & Scarrow 2003), but is inferred to be the general cause for mid-Cretaceous deformation and widespread terrane accretion.

"Continental" case

Figure 5 illustrates the situation for deformation associated with a superplume event where rising mantle plumes impact largely beneath continental lithosphere. Apart from some evidence for oceanic hotspot magmatism at 227 Ma (Lapierre *et al.*

2003) and 210 Ma (Kerr *et al.* 2000), most Late Triassic–Early Jurassic large igneous province magmatism and inferred mantle plume impacts affected the continents. Deformation associated with this putative superplume event we refer to as the "continental" case. In the pre-superplume state, as before, subducted oceanic lithosphere accumulates at the 670 km discontinuity, beneath subduction zones on the edges of a supercontinent. In Figure 5a the supercontinental margins are in tension (Hamilton 1994) as for the "oceanic" case. In Figure 5b a superplume event is inferred to initiate by the same process as outlined above, but with the variation that heat advection to, and uplift of, the upper mantle occurs beneath continental lithosphere. This results in adiabatic decompression melting and magmatism, as before, and generation of a broad, thermally generated topographic high. Gravitational sliding away from this high increases the coupling between continental lithosphere in the hanging wall of subduction zones and the subducting slab, and may result in over-riding of oceanic lithosphere by continental lithosphere, both of which combine to generate supercontinent margin deformation. At the same time, gravitational sliding away from the topographic high triggers the onset of supercontinental break-up. The temporal association between the onset of break-up and continent marginal compression provides support for active models of supercontinent break-up involving mantle plumes (Storey 1995) because passive models require plate margins to be in a state of tension. The environment of Late Triassic–Early Jurassic deformation is almost certainly made more complex by the presence of an effectively intra-continental palaeo-Tethyan ocean. The evidence for hotspot magmatism in this ocean in the Late Triassic (Okay *et al.* 2002) raises the possibility that a situation akin to the mid-Cretaceous "oceanic" case may also have

been active, subjecting Pangaea to a "double-whammy" from the point of view of superplume-related deformation.

Summary - a unifying mechanism

Oceanic and continental lithospheric plates appear to behave in similar ways when impacted from beneath by multiple plumes of hot rising mantle material. In terms of plate-marginal deformation in the Late Triassic–Early Jurassic and mid-Cretaceous, this can be summarized as the result of increased plate coupling at subduction zones during gravitational sliding of lithosphere away from broad, superplume-generated, thermally supported topographic highs. Evidence for Early Jurassic (Nakanishi *et al.* 1992) and late Early Cretaceous (Nakanishi & Winterer 1998; Sutherland & Hollis 2001) changes in palaeo-Pacific plate geometry, and Early Jurassic evidence for continental break-up or mid-Cretaceous periods of anomalous periods of extension, suggests that multiple plume impacts at the base of lithospheric plates are also likely to trigger plate reorganization. This is expressed as formation of new spreading ridges and the death of existing ones in the case of oceanic lithosphere, and continental break-up or high-rate extension in the case of continental lithosphere. Both can be described in terms of "break-up". "Oceanic break-up" (Fig. 4b) is comparable to continental break-up, but more subtly expressed, because breaking-up oceanic lithosphere, i.e. forming new spreading ridges, simply creates more oceanic lithosphere. Both can also be described in terms of plate reorganization: continental break-up can be viewed as plate reorganization of continental lithosphere. However, this break-up/reorganization relationship is the fundamental point that links mid-Cretaceous and Late Triassic–Early Jurassic deformation and that points to a unifying

mechanism for superplume–plate interactions. This can be summarized in the following sentence: when lithospheric plates are impacted from beneath by multiple plumes of hot rising mantle material they break-up/reorganize associated with gravitational spreading away from a broad, thermally generated topographic high and with a resulting short-lived pulse of plate-marginal deformation. This simple mechanism provides a unifying framework for continental and oceanic plate behaviour during the Late Triassic–Early Jurassic and mid-Cretaceous superplume events, explains episodicity of terrane accretion, and provides strong supporting evidence for active models of supercontinent break-up.

Conclusions

A review of evidence for deformation on the Late Triassic–Early Jurassic margins of Pangea and the mid-Cretaceous margins of the palaeo-Pacific ocean, and examination of the relationships between plate-marginal deformation and coeval probable superplume events, results in the following conclusions:

1. Late Triassic–Early Jurassic deformation is widely developed on the margins of Pangea (expressed as the Indosinian orogeny in Eurasia) and appears to have occurred in a short period between 202 Ma and 197 Ma.
2. Late Triassic–Early Jurassic deformation was coeval with eruption of the Central Atlantic Magmatic Province, onset of Pangea break-up, a longer than usual period of normal magnetic polarity in the Rhaetian–Hettangian and a major mass extinction event, all possible expressions of a superplume event.

3. Mid-Cretaceous deformation occurred in two brief periods, the first from ~116 Ma to ~110 Ma in the west palaeo-Pacific and the second from ~105 Ma to ~99 Ma in the east palaeo-Pacific, with both events possibly represented in northeast Siberia, and is also developed on the northern margin of neo-Tethys.

4. This deformation was coeval with eruption of major oceanic plateaus, extensional core-complex formation and rifting of New Zealand from Gondwana, the Cretaceous normal polarity epoch, and a major radiation of flowering plants and several animal groups (pollinating insects, birds, frogs, snakes, lizards, turtles, bryozoans and bivalves), all linked with the mid-Cretaceous superplume event.

5. Plate-marginal deformation in the Late Triassic–Early Jurassic and mid-Cretaceous can be conceptually modelled as the result of increased plate coupling at subduction zones during gravitational sliding of lithosphere away from superplume-generated, thermally supported topographic highs.

6. A simple unifying mechanism for superplume–plate interactions, and support for active models of supercontinent break-up, can be summarized thus: When large oceanic or continental plates are impacted from beneath by multiple plumes of hot rising mantle material they break-up/reorganize associated with gravitational spreading away from a thermally generated topographic high and with a resulting short-lived pulse of plate-marginal deformation, often associated with terrane accretion.

This is a contribution to the British Antarctic Survey Core Project "Superterrane in the Pacific-margin arc" (SPARC). The authors would like to thank Roger Larson, Brendan Murphy and Phil Leat for helpful and constructive reviews.

References

- Abbott, D.H. & Isley, A.E. 2002. The intensity, occurrence, and duration of superplume events and eras over geological time. *Journal of Geodynamics*, **34** (2), 265–307.
- Aberhan, M. & Fursich, F.T. 2000. Mass origination versus mass extinction: the biological contribution to the Pliensbachian–Toarcian extinction event. *Journal of the Geological Society, London*, **157** (1), 55–60.
- Acton, S.L., Simony, P.S. & Heaman, L.M. 2002. Nature of the basement to Quesnel Terrane near Christina Lake, southeastern British Columbia. *Canadian Journal of Earth Sciences*, **39** (1), 65–78.
- Adams, C.J., Barley, M.E., Maas, R. & Doyle, M.G. 2002. Provenance of Permian–Triassic volcanoclastic sedimentary terranes in New Zealand: evidence from their radiogenic isotope characteristics and detrital mineral age patterns. *New Zealand Journal of Geology and Geophysics*, **45** (2), 221–242.
- Adams, C.J. & Graham, I.J. 1996. Metamorphic and tectonic geochronology of the Torlesse Terrane, Wellington, New Zealand. *New Zealand Journal of Geology and Geophysics*, **39** (2), 157–180.
- Aitkenhead, N. 1975. *The geology of the Duse Bay-Larsen Inlet area, north-east Graham Land (with particular reference to the Trinity Peninsula Series)*. British Antarctic Survey Scientific Reports, **51**.
- Algeo, T.J. 1996. Geomagnetic polarity bias patterns through the Phanerozoic. *Journal of Geophysical Research-Solid Earth*, **101** (B2), 2785–2814.
- Algeo, T.J. & Sessler, K.B. 1995. The Paleozoic world: continental flooding, hypsometry, and sea-level. *American Journal of Science*, **295** (7), 787–822.
- Alroy, J. 2004. Are Sepkoski's evolutionary faunas dynamically coherent? *Evolutionary Ecology Research*, **6** (1), 1–32.
- Anderson, D.L. 1998. The scales of mantle convection. *Tectonophysics*, **284**, 1–17.
- Andrusevich, V.E., Engel, M.H., Zumberge, J.E. & Brothers, L.A. 1998. Secular, episodic changes in stable carbon isotope composition of crude oils. *Chemical Geology*, **152** (1-2), 59–72.
- Arakawa, Y., Saito, Y. & Amakawa, L. 2000. Crustal development of the Hida belt, Japan: evidence from Nd- Sr isotopic and chemical characteristics of igneous and metamorphic rocks. *Tectonophysics*, **328** (1-2), 183–204.
- Bambach, R.K. 1999. Energetics in the global marine fauna: a connection between terrestrial diversification and change in the marine biosphere. *Geobios*, **32** (2), 131–144.
- Barrio, C.A. & Coffield, D.Q. 1992. Late Cretaceous stratigraphy of the Upper Magdalena Basin in the Payandé-Chaparral segment (western Girardot Sub-Basin), Columbia. *Journal of South American Earth Sciences*, **5**, 123–139.
- Bartolini, A. & Larson, R.L. 2001. Pacific microplate and the Pangea supercontinent in the Early to Middle Jurassic. *Geology*, **29** (8), 735–738.

- Bassett, K.N. & Kleinspehn, K.L. 1996. Mid-Cretaceous transtension in the Canadian Cordillera: evidence from the Rocky Ridge volcanics of the Skeena group. *Tectonics*, **15** (4), 727–746.
- Beck, M.E., Jr., Burmester, R., Cembrano, J., Drake, R., Garcia, A., Hervé, F. & Munizaga, F. 2000. Paleomagnetism of the North Patagonian batholith, southern Chile: an exercise in shape analysis. *Tectonophysics*, **326** (1-2), 185–202.
- Beck, M.E., Jr. & Housen, B.A. 2003. Absolute velocity of North America during the Mesozoic from paleomagnetic data. *Tectonophysics*, **377** (1–2), 33–54.
- Beerling, D.J. & Berner, R.A. 2002. Biogeochemical constraints on the Triassic-Jurassic boundary carbon cycle event. *Global Biogeochemical Cycles*, **16** (3), 1–12, 1036, 10.1029/2001GB001637.
- Belousova, E.A., Griffin, W.L., Shee, S.R., Jackson, S.E. & O'Reilly, S.Y. 2001. Two age populations of zircons from the Timber Creek kimberlites, Northern Territory, as determined by laser-ablation ICP-MS analysis. *Australian Journal of Earth Sciences*, **48** (5), 757–765.
- Benton, M.J. 1996. Testing the roles of competition and expansion in tetrapod evolution. *Proceedings of the Royal Society of London, Series B*, **263** (1370), 641–646.
- Biggin, A.J. & Thomas, D.N. 2003. Analysis of long-term variations in the geomagnetic poloidal field intensity and evaluation of their relationship with global geodynamics. *Geophysical Journal International*, **152** (2), 392–415.
- Birkenmajer, K. 1994. Geology of Cretaceous magmatic rocks at Paradise Harbour, Danco Coast, Antarctic Peninsula. *Studia Geologica Polonica*, **104**, 7–39.
- Borrego, A.G., Hagemann, H.W., Blanco, C.G., Valenzuela, M. & deCenti, C.S. 1996. The Pliensbachian (Early Jurassic) "anoxic" event in Asturias, northern Spain: Santa Mera Member, Rodiles Formation. *Organic Geochemistry*, **25** (5-7), 295–309.
- Bradshaw, J.D. 1989. Cretaceous geotectonic patterns in the New Zealand region. *Tectonics*, **8**, 803–820.
- Bradshaw, J.D., Andrews, P.B. & Adams, C.J. 1981. Carboniferous to Cretaceous on the Pacific margin of Gondwana: the Rangitata Phase of New Zealand. In: Creswell, M.M. & Vella, P. (eds) *Gondwana Five: Papers and Abstracts of Papers Presented at the Fifth International Gondwana Symposium*. Balkema, Rotterdam, 217–221.
- Bradshaw, J.D., Weaver, S.D. & Muir, R.J. 1996. Mid-Cretaceous oroclinal bending of New Zealand terranes. *New Zealand Journal of Geology and Geophysics*, **39** (3), 461–468.
- Brown, M., Diaz, F. & Grocott, J. 1993. Displacement history of the Atacama fault system 25°00' S–27°00' S, northern Chile. *Geological Society of America Bulletin*, **105** (9), 1165–1174.
- Bruce, R.M., Nelson, E.P., Weaver, S.G. & Lux, D.R. 1991. Temporal and spatial variations in the southern Patagonian batholith: constraints on magmatic arc development. *Geological Society of America Special Papers*, **265**, 1–12.
- Bryan, S.E., Constantine, A.E., Stephens, C.J., Ewart, A., Schon, R.W. & Parianos, J. 1997. Early Cretaceous volcano-sedimentary successions along the eastern Australian continental margin: Implications for the break-up of eastern Gondwana. *Earth and Planetary Science Letters*, **153** (1-2), 85–102.
- Bryan, S.E., Ewart, A., Stephens, C.J., Parianos, J. & Downes, P.J. 2000. The Whitsunday Volcanic Province, Central Queensland, Australia: lithological

- and stratigraphic investigations of a silicic-dominated large igneous province. *Journal of Volcanology and Geothermal Research*, **99** (1-4), 55–78.
- Burn, R.W. 1984. *The geology of the LeMay Group, Alexander Island*. British Antarctic Survey Scientific Reports, **109**.
- Butler, R.F., Gehrels, G.E. & Saleeby, J.B. 2001. Paleomagnetism of the Duke Island, Alaska, ultramafic complex revisited. *Journal of Geophysical Research*, **106** (B9), 19259–19269.
- Butler, S. & Peltier, W.R. 1997. Internal thermal boundary layer stability in phase transition modulated convection. *Journal of Geophysical Research*, **102**, 2731–2749.
- Butterworth, P.J., Crame, J.A., Howlett, P.J. & Macdonald, D.I.M. 1988. Lithostratigraphy of Upper Jurassic–Lower Cretaceous strata of eastern Alexander Island, Antarctica. *Cretaceous Research*, **9**, 249–264.
- Campbell, R.J. & Haig, D.W. 1999. Bathymetric change during Early Cretaceous intracratonic marine transgression across the northeastern Eromanga Basin, Australia. *Cretaceous Research*, **20** (4), 403–446.
- Cantrill, D.J. 2000. A new macroflora from the South Orkney Islands, Antarctica: evidence of an Early to Middle Jurassic age for the Powell Island Conglomerate. *Antarctic Science*, **12** (2), 185–195.
- Carter, R.M. 1988. Post-breakup stratigraphy of the Kaikoura synthem (Cretaceous–Cenozoic), continental margin, southeastern New Zealand. *New Zealand Journal of Geology and Geophysics*, **31** (4), 405–429.
- Cecca, F. & Macchioni, F. 2004. The two Early Toarcian (Early Jurassic) extinction events in ammonoids. *Lethaia*, **37** (1), 35–56.
- Centeno-Garcia, E. & Keppie, J.D. 1999. Latest Paleozoic early Mesozoic structures in the central Oaxaca terrane of southern Mexico: deformation near a triple junction. *Tectonophysics*, **301** (3-4), 231–242.
- Chang, E.Z. 1996. Collisional orogenesis between North and South China and its eastern extension in the Korean peninsula. *Journal of Southeast Asian Earth Sciences*, **13** (3-5), 267–277.
- Chardon, D. 2003. Strain partitioning and batholith emplacement at the root of a transpressive magmatic arc. *Journal of Structural Geology*, **25** (1), 91–107.
- Charrier, R., Wyss, A.R., Flynn, J.J., Swisher, C.C., Norell, M.A., Zapatta, F., McKenna, M.C. & Novacek, M.J. 1996. New evidence for late Mesozoic early Cenozoic evolution of the Chilean Andes in the Upper Tinguiririca Valley (35° S), Central Chile. *Journal of South American Earth Sciences*, **9** (5-6), 393–422.
- Checa, A.G. & Jimenez-Jimenez, A.P. 2003. Evolutionary morphology of oblique ribs of bivalves. *Palaeontology*, **46**, 709–724.
- Chen, G., Grapes, R. & Zhang, K. 2003. A model for Mesozoic crustal melting and tectonic deformation in Southeast China. *International Geology Review*, **45** (10), 948–957.
- Chen, W.S., Yang, H.C., Wang, X. & Huang, H. 2002. Tectonic setting and exhumation history of the Pingtan–Dongshan Metamorphic Belt along the coastal area, Fujian Province, Southeast China. *Journal of Asian Earth Sciences*, **20** (7), 829–840.
- Clark, A.H., Farrar, E., Kontak, D.J., Langridge, R.J., Arenas, M.J., France, L.J., McBride, S.L., Woodman, P.L., Wasteneys, H.A., Sandeman, H.A. & Archibald, D.A. 1990. Geologic and geochronological constraints on the

- metallogenic evolution of the Andes of southeastern Peru. *Economic Geology and the Bulletin of the Society of Economic Geologists*, **85** (7), 1520–1583.
- Cluzel, D., Alles, W. & Lapiere, H. 1991. The Triassic–Jurassic calc-alkaline acidic intrusions of the Ogcheon Belt (South-Korea): continent-based arc or post-collisional magmatism. *Comptes Rendus de l'Academie Des Sciences Serie II*, **313** (4), 435–442.
- Coffin, M.F. & Eldholm, O. 1994. Large igneous provinces: crustal structure, dimensions, and external consequences. *Reviews of Geophysics*, **32**, 1–36.
- Cole, F., Bird, K.J., Toro, J., Roure, F., Osullivan, P.B., Pawlewicz, M. & Howell, D.G. 1997. An integrated model for the tectonic development of the frontal Brooks Range and Colville Basin 250 km west of the Trans-Alaska Crustal Transect. *Journal of Geophysical Research-Solid Earth*, **102** (B9), 20685–20706.
- Coleman, D.S., Briggs, A.S., Glazner, A.F. & Northrup, C.J. 2003. Timing of plutonism and deformation in the White Mountains of eastern California. *Geological Society of America Bulletin*, **115** (1), 48–57.
- Coleman, D.S., Gray, W. & Glazner, A.F. 2004. Rethinking the emplacement and evolution of zoned plutons: geochronologic evidence for incremental assembly of the Tuolumne Intrusive Suite, California. *Geology*, **32** (5), 433–436.
- Condie, K.C. 1998. Episodic continental growth and supercontinents: a mantle avalanche connection? *Earth and Planetary Science Letters*, **163**, 97–108.
- Condie, K.C. 2002. The supercontinent cycle: are there two patterns of cyclicity? *Journal of African Earth Sciences*, **35** (2), 179–183.
- Connolly, S.R. & Miller, A.I. 2002. Global Ordovician faunal transitions in the marine benthos: ultimate causes. *Paleobiology*, **28** (1), 26–40.
- Coombs, D.S., Landis, C.A., Norris, R.J., Sinton, J.M., Borns, D.J. & Craw, D. 1976. The Dun Mountain ophiolite belt, New Zealand, its tectonic setting, constitution, and origin, with special reference to the southern portion. *American Journal of Science*, **276**, 561–603.
- Courtillot, V.E. & Renne, P.R. 2003. On the ages of flood basalt events. *Comptes Rendus Geoscience*, **335** (1), 113–140.
- Cox, R.T. & Van Arsdale, R.B. 2002. The Mississippi Embayment, North America: a first order continental structure generated by the Cretaceous superplume mantle event. *Journal of Geodynamics*, **34** (2), 163–176.
- Crame, J.A. & Howlett, P.J. 1988. Late Jurassic and Early Cretaceous biostratigraphy of the Fossil Bluff Formation, Alexander Island. *British Antarctic Survey Bulletin*, **No. 78**, 1–35.
- Crowhurst, P.V., Maas, R., Hill, K.C., Foster, D.A. & Fanning, C.M. 2004. Isotopic constraints on crustal architecture and Permo-Triassic tectonics in New Guinea: possible links with eastern Australia. *Australian Journal of Earth Sciences*, **51** (1), 107–122.
- Cunningham, W.D. 1995. Orogenesis at the southern tip of the Americas: the structural evolution of the Cordillera Darwin metamorphic complex, southernmost Chile. *Tectonophysics*, **244** (4), 197–229.
- Curtis, M.L. 2001. Tectonic history of the Ellsworth Mountains, West Antarctica: reconciling a Gondwana enigma. *Geological Society of America Bulletin*, **113** (7), 939–958.
- Curtis, M.L. 2002. Palaeozoic to Mesozoic polyphase deformation of the Patuxent Range, Pensacola Mountains, Antarctica. *Antarctic Science*, **14** (2), 175–183.

- Dalziel, I.W.D. 1981. Back-arc extension in the southern Andes: a review and critical appraisal. *Philosophical Transactions of the Royal Society, London, Series A*, **300**, 319–395.
- Dalziel, I.W.D. 1982. The early (pre-Middle Jurassic) history of the Scotia Arc region: a review and progress report. In: Craddock, C. (ed.) *Antarctic Science*. University of Wisconsin Press, Madison, 111–126.
- Dalziel, I.W.D. 1986. Collision and Cordilleran orogenesis: an Andean perspective. In: Coward, M.P. & Ries, A.C. (eds) *Collision Tectonics*. Geological Society, London, Special Publications, **19**, 389–404.
- Del Valle, R.A. & Miller, H. 2001. Transpressional deformation along the margin of Larsen Basin: new data from Pedersen Nunatak, Antarctic Peninsula. *Antarctic Science*, **13** (2), 158–166.
- Delteil, J., Stephan, J.F., de Lepinay, B.M. & Ruellan, E. 2003. Wrench tectonics flip at oblique subduction. A model from New Zealand. *Comptes Rendus Geoscience*, **335** (9), 743–750.
- Dickinson, W.R. & Lawton, T.F. 2001. Carboniferous to Cretaceous assembly and fragmentation of Mexico. *Geological Society of America Bulletin*, **113** (9), 1142–1160.
- Dixon, J. 1993. Regional unconformities in the Cretaceous of North-West Canada. *Cretaceous Research*, **14** (1), 17–38.
- Dixon, J. 1997. Cretaceous stratigraphy in the subsurface of Great Slave Plain, southern Northwest Territories. *Bulletin of Canadian Petroleum Geology*, **45** (2), 178–&.
- Doblas, M., Oyarzun, R., Lopez-Ruiz, J., Cebria, J.M., Youbi, N., Mahecha, V., Lago, M., Pocovi, A. & Cabanis, B. 1998. Permo-Carboniferous volcanism in Europe and northwest Africa: a superplume exhaust valve in the centre of Pangaea? *Journal of African Earth Sciences*, **26** (1), 89–99.
- Dott, R.H., Jr., Winn, R.D., Jr., de Wit, M.J. & Bruhn, R.L. 1977. Tectonic and sedimentary significance of Cretaceous Tekenika Beds of Tierra del Fuego. *Nature*, **266**, 620–622.
- Doubleday, P.A., Macdonald, D.I.M. & Nell, P.A.R. 1993. Sedimentology and structure of the trench-slope to fore-arc basin transition in the Mesozoic of Alexander Island, Antarctica. *Geological Magazine*, **130** (6), 737–754.
- Doubleday, P.A. & Storey, B.C. 1998. Deformation history of a Mesozoic forearc basin sequence on Alexander Island, Antarctic Peninsula. *Journal of South American Earth Sciences*, **11**, 1–21.
- Dobrovine, P.V. & Tarduno, J.A. 2004. Self-reversed magnetization carried by titanomagnetite in oceanic basalts. *Earth and Planetary Science Letters*, **222** (3-4), 959-969.
- Draper, G., Gutierrez, G. & Lewis, J.F. 1996. Thrust emplacement of the Hispaniola peridotite belt: orogenic expression of the mid-Cretaceous Caribbean arc polarity reversal? *Geology*, **24** (12), 1143–1146.
- Ernst, W.G. 1993. Metamorphism of Franciscan tectonostratigraphic assemblage, Pacheco Pass area, east-central Diablo Range, California Coast Ranges. *Geological Society of America Bulletin*, **105** (5), 618–636.
- Evenchick, C.A. & McNicoll, V.J. 2002. Stratigraphy, structure, and geochronology of the Anyox Pendant, northwest British Columbia, and implications for mineral exploration. *Canadian Journal of Earth Sciences*, **39** (9), 1313–1332.

- Faure, M., Marchadier, Y. & Rangin, C. 1989. Pre-Eocene synmetamorphic structure in the Mindoro-Romblon- Palawan Area, West Philippines, and implications for the history of Southeast-Asia. *Tectonics*, **8** (5), 963–979.
- Faure, M., Natalin, B.A., Monie, P., Vrublevsky, A.A., Borukaiev, C. & Prikhodko, V. 1995. Tectonic evolution of the Anuy metamorphic rocks (Sikhote-Alin, Russia) and their place in the Mesozoic geodynamic framework of east Asia. *Tectonophysics*, **241** (3-4), 279–301.
- Filatova, N.I. & Vishnevskaya, V.S. 1997. Radiolarian stratigraphy and origin of the Mesozoic terranes of the continental framework of the northwestern Pacific (Russia). *Tectonophysics*, **269** (1-2), 131–150.
- Fisk, M. & Kelley, K.A. 2002. Probing the Pacific's oldest MORB glass: mantle chemistry and melting conditions during the birth of the Pacific Plate. *Earth and Planetary Science Letters*, **202** (3-4), 741–752.
- Foden, J., Song, S.H., Turner, S., Elburg, M., Smith, P.B., Van der Steldt, B. & Van Penglis, D. 2002. Geochemical evolution of lithospheric mantle beneath SE South Australia. *Chemical Geology*, **182** (2-4), 663–695.
- Gaetani, M. 1997. The Karakorum Block in Central Asia, from Ordovician to Cretaceous. *Sedimentary Geology*, **109** (3-4), 339–359.
- Gallet, Y. & Hulot, G. 1997. Stationary and nonstationary behaviour within the geomagnetic polarity time scale. *Geophysical Research Letters*, **24** (15), 1875–1878.
- George, A.D. 1993. Radiolarians in offscraped seamount fragments, Aorangi Range, New Zealand. *New Zealand Journal of Geology and Geophysics*, **36** (2), 185–199.
- George, A.D., Marshallsea, S.J., Wyrwoll, K.H., Chen, J. & Lu, Y.C. 2001. Miocene cooling in the northern Qilian Shan, northeastern margin of the Tibetan Plateau, revealed by apatite fission-track and vitrinite-reflectance analysis. *Geology*, **29** (10), 939–942.
- Golonka, J. 2004. Plate tectonic evolution of the southern margin of Eurasia in the Mesozoic and Cenozoic. *Tectonophysics*, **381** (1-4), 235–273.
- Gradstein, F.M., Ogg, J.G., Smith, A.G. and 36 others 2004. *A Geologic Time Scale 2004*. Cambridge University Press, Cambridge.
- Grimaldi, D. 1999. The co-radiations of pollinating insects and angiosperms in the Cretaceous. *Annals of the Missouri Botanical Garden*, **86** (2), 373–406.
- Grocott, J. & Taylor, G.K. 2002. Magmatic arc fault systems, deformation partitioning and emplacement of granitic complexes in the Coastal Cordillera, north Chilean Andes (25°30' S to 27°00' S). *Journal of the Geological Society*, **159**, 425–442.
- Grunow, A.M., Dalziel, I.W.D., Harrison, T.M. & Heizler, M.T. 1992. Structural geology and geochronology of subduction complexes along the margin of Gondwanaland: new data from the Antarctic Peninsula and southernmost Andes. *Geological Society of America Bulletin*, **104** (11), 1497–1514.
- Guex, J., Bartolini, A., Atudorei, V. & Taylor, D. 2004. High-resolution ammonite and carbon isotope stratigraphy across the Triassic–Jurassic boundary at New York Canyon (Nevada). *Earth and Planetary Science Letters*, **in press**.
- Haas, J. & Pero, C. 2004. Mesozoic evolution of the Tisza Mega-unit. *International Journal of Earth Sciences*, **93** (2), 297–313.
- Haig, D.W. & Lynch, D.A. 1993. A late early Albian marine transgressive pulse over northeastern Australia, precursor to epeiric basin anoxia: foraminiferal evidence. *Marine Micropaleontology*, **22** (4), 311–362.

- Hall, L.S., Lamb, S.H. & Mac Niocaill, C. 2004. Cenozoic distributed rotational deformation, South Island, New Zealand. *Tectonics*, **23** (3), 1–16, TC2002, 10.1029/2002TC001421.
- Hallam, A. & Wignall, P.B. 1999. Mass extinctions and sea-level changes. *Earth-Science Reviews*, **48** (4), 217–250.
- Halpern, M. & Rex, D.C. 1972. Time of folding of the Yahgan formation and age of the Teckenika bed, southern Chile, South America. *Geological Society of America Bulletin*, **83**, 1881–1886.
- Hamilton, W.B. 1994. Subduction systems and magmatism. In: Smellie, J.L. (ed.) *Volcanism associated with extension at consuming plate margins*. Geological Society, London, Special Publications, **81**, 3–28.
- Handoh, I.C. & Lenton, T.M. 2003. Periodic mid-Cretaceous oceanic anoxic events linked by oscillations of the phosphorus and oxygen biogeochemical cycles. *Global Biogeochemical Cycles*, **17** (4), 1–13, 1092, 10.1029/2003GB002039.
- Hansen, V.L. & Dusel-Bacon, C. 1998. Structural and kinematic evolution of the Yukon–Tanana upland tectonites, east-central Alaska: a record of late Paleozoic to Mesozoic crustal assembly. *Geological Society of America Bulletin*, **110** (2), 211–230.
- Haq, B.U., Hardenbol, J. & Vail, P.R. 1987. Chronology of fluctuating sea-levels since the Triassic. *Science*, **235**, 1156–1167.
- Harlow, G.E., Hemming, S.R., Lallemand, H.G.A., Sisson, V.B. & Sorensen, S.S. 2004. Two high-pressure-low-temperature serpentinite-matrix melange belts, Motagua fault zone, Guatemala: a record of Aptian and Maastrichtian collisions. *Geology*, **32** (1), 17–20.
- Harries, P.J. & Little, C.T.S. 1999. The early Toarcian (Early Jurassic) and the Cenomanian-Turonian (Late Cretaceous) mass extinctions: similarities and contrasts. *Palaeogeography Palaeoclimatology Palaeoecology*, **154**, 39–66.
- Harrington, H.J. & Korsch, R.J. 1985. Late Permian to Cainozoic tectonics of the New England Orogen. *Australian Journal of Earth Sciences*, **32**, 181–203.
- Harris, M.J., Symons, D.T.A., Blackburn, W.H., Hart, C.J.R. & Villeneuve, M. 2003. Travels of the Cache Creek Terrane: a paleomagnetic, geobarometric and $^{40}\text{Ar}/^{39}\text{Ar}$ study of the Jurassic Fourth of July Batholith, Canadian Cordillera. *Tectonophysics*, **362** (1-4), 137–159.
- Hathway, B. 2000. Continental rift to back-arc basin: Jurassic–Cretaceous stratigraphical and structural evolution of the Larsen Basins, Antarctic Peninsula. *Journal of the Geological Society, London*, **157** (2), 417–432.
- Heaman, L.M. & Kjarsgaard, B.A. 2000. Timing of eastern North American kimberlite magmatism: continental extension of the Great Meteor hotspot track? *Earth and Planetary Science Letters*, **178** (3-4), 253–268.
- Heaman, L.M., Kjarsgaard, B.A. & Creaser, R.A. 2003. The timing of kimberlite magmatism in North America: implications for global kimberlite genesis and diamond exploration. *Lithos*, **71** (2-4), 153–184.
- Henderson, R.A. 1998. Eustatic and palaeoenvironmental assessment of the mid-Cretaceous Bathurst Island Group of the Money Shoals platform, northern Australia. *Palaeogeography Palaeoclimatology Palaeoecology*, **138** (1-4), 115–138.
- Hennessy, J.F. & Mossman, D.J. 1996. Geochemistry of Ordovician black shales at Meductic, southern Miramichi Highlands, New Brunswick. *Atlantic Geology*, **32** (3), 233–245.

- Hervé, F. & Fanning, C.M. 2001. Late Triassic detrital zircons in meta-turbidites of the Chonos Metamorphic Complex, southern Chile. *Revista Geologica De Chile*, **28** (1), 91–104.
- Hervé, F., Fanning, C.M. & Pankhurst, R.J. 2003. Detrital zircon age patterns and provenance of the metamorphic complexes of southern Chile. *Journal of South American Earth Sciences*, **16** (1), 107–123.
- Hesselbo, S.P., Grocke, D.R., Jenkyns, H.C., Bjerrum, C.J., Farrimond, P., Bell, H.S.M. & Green, O.R. 2000. Massive dissociation of gas hydrate during a Jurassic oceanic anoxic event. *Nature*, **406** (6794), 392–395.
- Hesselbo, S.P., Morgans-Bell, H.S., McElwain, J.C., Rees, P.M., Robinson, S.A. & Ross, C.E. 2003. Carbon-cycle perturbation in the Middle Jurassic and accompanying changes in the terrestrial paleoenvironment. *Journal of Geology*, **111** (3), 259–276.
- Hesselbo, S.P., Robinson, S.A. & Surlyk, F. 2004. Sea-level change and facies development across potential Triassic-Jurassic boundary horizons, SW Britain. *Journal of the Geological Society, London*, **161**, 365–379.
- Hesselbo, S.P., Robinson, S.A., Surlyk, F. & Piasecki, S. 2002. Terrestrial and marine extinction at the Triassic–Jurassic boundary synchronized with major carbon cycle perturbation: a link to initiation of massive volcanism? *Geology*, **30** (3), 251–254.
- Holdsworth, B.K. & Nell, P.A.R. 1992. Mesozoic radiolarian faunas from the Antarctic Peninsula: age, tectonic and paleoceanographic significance. *Journal of the Geological Society, London*, **149**, 1003–1020.
- Il'ina, V.I. & Shurygin, B.N. 2000. The Ilansk formation and its stratotype (Lower Jurassic, southern Siberia). *Geologiya I Geofizika*, **41** (8), 1195–1202.
- Ineson, J.R. 1985. Submarine glide blocks from the Lower Cretaceous of the Antarctic Peninsula. *Sedimentology*, **32** (5), 659–670.
- Ineson, J.R. 1989. Coarse-grained submarine fan and slope apron deposits in a Cretaceous back-arc basin, Antarctica. *Sedimentology*, **36** (5), 793–819.
- Inger, S., Scott, R.A. & Golionko, B.G. 1999. Tectonic evolution of the Taimyr Peninsula, northern Russia: implications for Arctic continental assembly. *Journal of the Geological Society, London*, **156**, 1069–1072.
- Isozaki, Y. & Itaya, T. 1990. Chronology of Sambagawa metamorphism. *Journal of Metamorphic Geology*, **8** (4), 401–411.
- Jablonski, D. & Chaloner, W.G. 1994. Extinctions in the fossil record. *Philosophical Transactions of the Royal Society of London Series B*, **344** (1307), 11–16.
- Jablonski, D., Lidgard, S. & Taylor, P.D. 1997. Comparative ecology of bryozoan radiations: Origin of novelties in cyclostomes and cheilostomes. *Palaios*, **12** (6), 505–523.
- Jacques, J.M. 2003a. A tectonostratigraphic synthesis of the Sub-Andean basins: implications for the geotectonic segmentation of the Andean Belt. *Journal of the Geological Society, London*, **160** (5), 687–701.
- Jacques, J.M. 2003b. A tectonostratigraphic synthesis of the Sub-Andean basins: inferences on the position of South American intraplate accommodation zones and their control on South Atlantic opening. *Journal of the Geological Society, Dublin*, **160** (5), 703–717.
- Jahren, A.H. 2002. The biogeochemical consequences of the mid-Cretaceous superplume. *Journal of Geodynamics*, **34** (2), 177–191.

- Jenkyns, H.C., Grocke, D.R. & Hesselbo, S.P. 2001. Nitrogen isotope evidence for water mass denitrification during the early Toarcian (Jurassic) oceanic anoxic event. *Paleoceanography*, **16** (6), 593–603.
- Johnson, C. & Gallagher, K. 2000. A preliminary Mesozoic and Cenozoic denudation history of the North East Greenland onshore margin. *Global and Planetary Change*, **24** (3-4), 261–274.
- Johnson, C.L. 2004. Polyphase evolution of the East Gobi basin: sedimentary and structural records of Mesozoic–Cenozoic intraplate deformation in Mongolia. *Basin Research*, **16** (1), 79–99.
- Johnson, H.P., Vanpatten, D., Tivey, M. & Sager, W.W. 1995. Geomagnetic polarity reversal rate for the Phanerozoic. *Geophysical Research Letters*, **22** (3), 231–234.
- Johnson, S.E., Tate, M.C. & Fanning, C.M. 1999. New geologic mapping and SHRIMP U-Pb zircon data in the Peninsular Ranges batholith, Baja California, Mexico: Evidence for a suture? *Geology*, **27** (8), 743–746.
- Jolivet, M., Brunel, M., Seward, D., Xu, Z., Yang, J., Roger, F., Tapponnier, P., Malavieille, J., Arnaud, N. & Wu, C. 2001. Mesozoic and Cenozoic tectonics of the northern edge of the Tibetan plateau: fission-track constraints. *Tectonophysics*, **343** (1-2), 111–134.
- Journey, J.M. & Friedman, R.M. 1993. The Coast Belt thrust system: evidence of Late Cretaceous shortening in southwest British Columbia. *Tectonics*, **12** (3), 756–775.
- Kamei, A., Owada, M., Hamamoto, T., Osanai, Y., Yuhara, M. & Kagami, H. 2000. Isotopic equilibration ages for the Miyanojima tonalite from the Higo metamorphic belt in central Kyushu, Southwest Japan: implications for the tectonic setting during the Triassic. *Island Arc*, **9** (1), 97–112.
- Kamp, P.J.J. 2000. Thermochronology of the Torlesse accretionary complex, Wellington region, New Zealand. *Journal of Geophysical Research*, **105** (B8), 19253–19272.
- Kazmin, V.G. 1991. Collision and rifting in the Tethys Ocean: geodynamic implications. *Tectonophysics*, **196** (3-4), 371–384.
- Kear, D. & Mortimer, N. 2003. Waipa Supergroup, New Zealand: a proposal. *Journal of the Royal Society of New Zealand*, **33** (1), 149–163.
- Kellogg, K.S. & Rowley, P.D. 1989. Structural geology and tectonics of the Orville Coast region, southern Antarctica Peninsula, Antarctica. *U.S. Geological Survey Professional Papers*, **1498**, 25.
- Kelly, S.R.A., Doubleday, P.A., Brunton, C.H.C., Dickins, J.M., Sevastopulo, G.D. & Taylor, P.D. 2001. First Carboniferous and ?Permian marine macrofaunas from Antarctica and their tectonic implications. *Journal of the Geological Society, London*, **158** (2), 219–232.
- Kent, D.V. & Olsen, P.E. 1999. Astronomically tuned geomagnetic polarity timescale for the Late Triassic. *Journal of Geophysical Research*, **104** (B6), 12831–12841.
- Kerr, A.C., Iturralde-Vinent, M.A., Saunders, A.D., Babbs, T.L. & Tarney, J. 1999. A new plate tectonic model of the Caribbean: implications from a geochemical reconnaissance of Cuban Mesozoic volcanic rocks. *Geological Society of America Bulletin*, **111** (11), 1581–1599.
- Kerr, A.C., White, R.V. & Saunders, A.D. 2000. LIP reading: Recognizing oceanic plateaux in the geological record. *Journal of Petrology*, **41** (7), 1041–1056.

- Kidder, D.L. & Worsley, T.R. 2004. Causes and consequences of extreme Permo-Triassic warming to globally equable climate and relation to the Permo-Triassic extinction and recovery. *Palaeogeography Palaeoclimatology Palaeoecology*, **203** (3-4), 207–237.
- Kimbrough, D.L., Smith, D.P., Mahoney, J.B., Moore, T.E., Grove, M., Gastil, R.G., Ortega-Rivera, A. & Fanning, C.M. 2001. Forearc-basin sedimentary response to rapid Late Cretaceous batholith emplacement in the Peninsular Ranges of southern and Baja California. *Geology*, **29** (6), 491–494.
- Kimura, G. 1997. Cretaceous episodic growth of the Japanese Islands. *Island Arc*, **6** (1), 52–68.
- Kimura, G., Sakakibara, M. & Okamura, M. 1994. Plumes in central Panthalassa: deductions from accreted oceanic fragments in Japan. *Tectonics*, **13** (4), 905–916.
- Kirichkova, A.I., Kostina, E.I. & Timoshina, N.A. 2003. Comprehensive substantiation of Jurassic phytostratigraphy and correlations in the Kansk coal basin, Siberia. *Stratigraphy and Geological Correlation*, **11** (3), 244–260.
- Kirichkova, A.I. & Kulikova, N.K. 2002. Correlation of different-facies Triassic deposits of the eastern Urals and Siberia. *Stratigraphy and Geological Correlation*, **10** (5), 488–502.
- Kirichkova, A.I. & Travina, T.A. 2000. Phytostratigraphy of Jurassic coal-bearing formations of the Irkutsk Basin. *Stratigraphy and Geological Correlation*, **8** (6), 608–620.
- Kiyokawa, S. 1992. Geology of the Idonnappu Belt, Central Hokkaido, Japan - evolution of a Cretaceous accretionary complex. *Tectonics*, **11** (6), 1180–1206.
- Klepeis, K.A., Clarke, G.L., Gehrels, G. & Vervoort, J. 2004. Processes controlling vertical coupling and decoupling between the upper and lower crust of orogens: results from Fiordland, New Zealand. *Journal of Structural Geology*, **26** (4), 765–791.
- Kohn, M.J., Spear, F.S. & Dalziel, I.W.D. 1993. Metamorphic P–T paths from Cordillera Darwin, a core complex in Tierra del Fuego, Chile. *Journal of Petrology*, **34** (3), 519–542.
- Kopylova, M.G., Russell, J.K. & Cookenboo, H. 1998. Upper-mantle stratigraphy of the Slave craton, Canada: insights into a new kimberlite province. *Geology*, **26** (4), 315–318.
- Kraemer, P.E. 2003. Orogenic shortening and the origin of the Patagonian orocline (56° S). *Journal of South American Earth Sciences*, **15** (7), 731–748.
- Kress, W.J., Prince, L.M., Hahn, W.J. & Zimmer, E.A. 2001. Unravelling the evolutionary radiation of the families of the Zingiberales using morphological and molecular evidence. *Systematic Biology*, **50** (6), 926–944.
- Kumar, A., Dayal, A.M. & Padmakumari, V.M. 2003. Kimberlite from Rajmahal magmatic province: Sr-Nd-Pb isotopic evidence for Kerguelen plume derived magmas. *Geophysical Research Letters*, **30** (24), 1–4, 2296, 10.1029/2003GL018518.
- Kusky, T.M. & Bradley, D.C. 1999. Kinematic analysis of melange fabrics: examples and applications from the McHugh Complex, Kenai Peninsula, Alaska. *Journal of Structural Geology*, **21** (12), 1773–1796.
- Laird, M.G. & Bradshaw, J.D. 2004. The break-up of a long-term relationship: the Cretaceous separation of New Zealand from Gondwana. *Gondwana Research*, **7** (1), 273–286.

- Lapierre, H., Bosch, D., Tardy, M. & Struik, L.C. 2003. Late Paleozoic and Triassic plume-derived magmas in the Canadian Cordillera played a key role in continental crust growth. *Chemical Geology*, **201** (1-2), 55–89.
- Lapierre, H., Jahn, B.M., Charvet, J. & Yu, Y.W. 1997. Mesozoic felsic arc magmatism and continental olivine tholeiites in Zhejiang province and their relationship with the tectonic activity in southeastern China. *Tectonophysics*, **274** (4), 321–338.
- Larson, R.L. 1991a. Geological consequences of superplumes. *Geology*, **19** (10), 963–966.
- Larson, R.L. 1991b. Latest pulse of Earth: evidence for a mid-Cretaceous superplume. *Geology*, **19** (6), 547–550.
- Larson, R.L. 1992. Latest pulse of Earth: evidence for a mid-Cretaceous superplume and geological consequences of superplumes - Reply. *Geology*, **20** (5), 476–477.
- Larson, R.L. 1997. Superplumes and ridge interactions between Ontong Java and Manihiki plateaus and the Nova-Canton trough. *Geology*, **25** (9), 779–782.
- Larson, R.L. & Erba, E. 1999. Onset of the mid-Cretaceous greenhouse in the Barremian–Aptian: Igneous events and the biological, sedimentary, and geochemical responses. *Paleoceanography*, **14** (6), 663–678.
- Larson, R.L. & Kincaid, C. 1996. Onset of mid-Cretaceous volcanism by elevation of the 670 km thermal boundary layer. *Geology*, **24** (6), 551–554.
- Laudon, T.S. & Fanning, C.M. 2003. SHRIMP U-Pb age characteristics of detrital and magmatic zircons, eastern Ellsworth Land, Abstracts of 9th International Symposium of Antarctic Earth Sciences, Potsdam, 156.
- Laudon, T.S., Thomson, M.R.A., Williams, P.L., Miliken, K.L., Rowley, P.D. & Boyles, J.M. 1983. The Jurassic Latady Formation, southern Antarctic Peninsula. In: Oliver, R., James, P.R. & Jago, J.B. (eds) *Antarctic Earth Science*. Australian Academy of Science, Canberra, 398–414.
- Lebron, M.C. & Perfit, M.R. 1993. Stratigraphic and petrochemical data support subduction polarity reversal of the Cretaceous Caribbean island arc. *Journal of Geology*, **101** (3), 389–396.
- Leckie, R.M., Bralower, T.J. & Cashman, R. 2002. Oceanic anoxic events and plankton evolution: Biotic response to tectonic forcing during the mid-Cretaceous. *Paleoceanography*, **17** (3), 1–12, 1041, 10.1029/2001PA000623.
- Lehmann, D., Brett, C.E., Cole, R. & Baird, G. 1995. Distal sedimentation in a peripheral foreland basin: Ordovician black shales and associated flysch of the western Taconic foreland, New York State and Ontario. *Geological Society of America Bulletin*, **107** (6), 708–724.
- Lepvrier, C., Maluski, H., Van Vuong, N., Rogues, D., Axente, V. & Rangin, C. 1997. Indosinian NW-trending shear zones within the Truong Son belt (Vietnam) $^{40}\text{Ar}/^{39}\text{Ar}$ Triassic ages and Cretaceous to Cenozoic overprints. *Tectonophysics*, **283** (1-4), 105–127.
- Leverenz, A. & Ballance, P.F. 2001. Terrane affiliation and terrane boundaries of Mesozoic accretionary complexes, northeastern North Island, New Zealand: some implications from recycled clastics. *New Zealand Journal of Geology and Geophysics*, **44** (4), 589–599.
- Li, X.H., Chen, Z., Liu, D.Y. & Li, W.X. 2003. Jurassic gabbro–granite–syenite suites from southern Jiangxi province, SE China: age, origin, and tectonic significance. *International Geology Review*, **45** (10), 898–921.

- Little, C.T.S. & Benton, M.J. 1995. Early Jurassic mass extinction: a global long-term event. *Geology*, **23** (6), 495–498.
- Little, T.A., Mortimer, N. & McWilliams, M. 1999. An episodic Cretaceous cooling model for the Otago–Marlborough Schist, New Zealand, based on $^{40}\text{Ar}/^{39}\text{Ar}$ white mica ages. *New Zealand Journal of Geology and Geophysics*, **42** (3), 305–325.
- Livermore, R.A. & Woollett, R.W. 1993. Sea-floor spreading in the Weddell Sea and southwest Atlantic since the Late Cretaceous. *Earth and Planetary Science Letters*, **117** (3-4), 475-495.
- Lu, H., Jia, D., Wang, Z., Guo, L., Shi, Y. & Zhang, Q. 1994. Tectonic evolution of the Dongshan Terrane, Fujian Province, China. *Journal of South American Earth Sciences*, **7** (3-4), 349–365.
- Lundin, E.R. & Dore, A.G. 1997. A tectonic model for the Norwegian passive margin with implications for the NE Atlantic: Early Cretaceous to break-up. *Journal of the Geological Society, London*, **154**, 545–550.
- Lupia, R. 1999. Discordant morphological disparity and taxonomic diversity during the Cretaceous angiosperm radiation: North American pollen record. *Paleobiology*, **25** (1), 1–28.
- Luyendyk, B.P. 1995. Hypothesis for Cretaceous rifting of East Gondwana caused by subducted slab capture. *Geology*, **23** (4), 373–376.
- MacDonald, A.J., Lewis, P.D., Thompson, J.F.H., Nadaraju, G., Bartsch, R.D., Bridge, D.J., Rhys, D.A., Roth, T., Kaip, A., Godwin, C.I. & Sinclair, A.J. 1996. Metallogeny of an early to middle Jurassic arc, Iskut river area, northwestern British Columbia. *Economic Geology and the Bulletin of the Society of Economic Geologists*, **91** (6), 1098–1114.
- Macdonald, D.I.M. & Butterworth, P.J. 1990. The stratigraphy, setting and hydrocarbon potential of the Mesozoic sedimentary basins of the Antarctic Peninsula. In: St. John, B. (ed.) *Antarctica as an Exploration Frontier*. Studies in Geology. American Association of Petroleum Geologists, **31**, 102–125.
- Macdonald, D.I.M., Storey, B.C. & Thomson, J.W. 1987. *South Georgia*. BAS GEOMAP Series, Sheet 1, 1:250000, Geological map and supplementary text. British Antarctic Survey, Cambridge.
- Macellari, C.E. 1988. Cretaceous palaeogeography and depositional cycles of western South America. *Journal of South American Earth Sciences*, **1**, 373–418.
- Machetel, P. 2003. Global thermal and dynamical perturbations due to Cretaceous mantle avalanche. *Comptes Rendus Geoscience*, **335** (1), 91–97.
- MacIntyre, D.G. & Villeneuve, M.E. 2001. Geochronology of mid-Cretaceous to Eocene magmatism, Babine porphyry copper district, central British Columbia. *Canadian Journal of Earth Sciences*, **38** (4), 639–655.
- Mahan, K.H., Bartley, J.M., Coleman, D.S., Glazner, A.F. & Carl, B.S. 2003. Sheeted intrusion of the synkinematic McDoogle pluton, Sierra Nevada, California. *Geological Society of America Bulletin*, **115** (12), 1570–1582.
- Maher, H.D. 2001. Manifestations of the Cretaceous High Arctic large igneous province in Svalbard. *Journal of Geology*, **109** (1), 91–104.
- Malavieille, J., Chemenda, A. & Larroque, C. 1998. Evolutionary model for Alpine Corsica: mechanism for ophiolite emplacement and exhumation of high-pressure rocks. *Terra Nova*, **10** (6), 317–322.
- Mambole, A. & Fleitout, L. 2002. Petrological layering induced by an endothermic phase transition in the Earth's mantle. *Geophysical Research Letters*, **29** (22), 1–4, 2044, 10.1029/2002GL014674.

- Marshallsea, S.J., Green, P.F. & Webb, J. 2000. Thermal history of the Hodgkinson Province and Laura Basin, Queensland: multiple cooling episodes identified from apatite fission track analysis and vitrinite reflectance data. *Australian Journal of Earth Sciences*, **47** (4), 779–797.
- Martin, M.W., Kato, T.T., Rodriguez, C., Godoy, E., Duhart, P., McDonough, M. & Campos, A. 1999. Evolution of the late Paleozoic accretionary complex and overlying forearc-magmatic arc, south central Chile (38° S–41° S): Constraints for the tectonic setting along the southwestern margin of Gondwana. *Tectonics*, **18** (4), 582–605.
- Marzoli, A., Renne, P.R., Piccirillo, E.M., Ernesto, M., Bellieni, G. & De Min, A. 1999. Extensive 200-million-year-old continental flood basalts of the Central Atlantic Magmatic Province. *Science*, **284** (5414), 616–618.
- McElhinny, M.W. & Larson, R.L. 2003. Jurassic dipole low defined from land and sea data. *Eos*, **84** (37), 362–366.
- McNulty, B.A. 1995. Shear zone development during magmatic arc construction: the Bench Canyon shear zone, central Sierra Nevada, California. *Geological Society of America Bulletin*, **107** (9), 1094–1107.
- Mégard, F. 1984. The Andean orogenic period and its major structures in central and northern Peru. *Journal of the Geological Society, London*, **141** (5), 893–900.
- Meneilly, A.W. 1983. Deformation of granitic plutons in eastern Palmer Land. *British Antarctic Survey Bulletin*, **No. 61**, 75–79.
- Meneilly, A.W. 1988. Reverse-fault step at Engel Peaks, Antarctic Peninsula. *Journal of Structural Geology*, **10** (4), 393–403.
- Meng, Q.R. & Zhang, G.W. 2000. Geologic framework and tectonic evolution of the Qinling orogen, central China. *Tectonophysics*, **323** (3-4), 183–196.
- Metcalf, I. 2000. The Bentong-Raub Suture Zone. *Journal of Asian Earth Sciences*, **18** (6), 691–712.
- Millar, I.L., Pankhurst, R.J. & Fanning, C.M. 2002. Basement chronology of the Antarctic Peninsula: recurrent magmatism and anatexis in the Palaeozoic Gondwana Margin. *Journal of the Geological Society, London*, **159**, 145–157.
- Miller, H. 1983. The position of Antarctica within Gondwana in the light of Palaeozoic orogenic development. In: Oliver, R.L., James, P.R. & Jago, J.B. (eds) *Antarctic Earth Science*. Australian Academy of Science, Canberra, 579–581.
- Monie, P., Soliva, J., Brunel, M. & Maluski, H. 1994. Mylonitic shear zones in the Millas Granite (Pyrenees, France): ⁴⁰Ar/³⁹Ar Cretaceous ages and tectonic interpretation. *Bulletin de la Societe Geologique de France*, **165** (6), 559–571.
- Mortimer, N. 1986. Late Triassic, arc-related, potassic igneous rocks in the North American Cordillera. *Geology*, **14** (12), 1035–1038.
- Mortimer, N. 1987. The Nicola-Group - Late Triassic and Early Jurassic subduction-related volcanism in British-Columbia. *Canadian Journal of Earth Sciences*, **24** (12), 2521–2536.
- Mortimer, N. 1993. Jurassic tectonic history of the Otago Schist, New Zealand. *Tectonics*, **12** (1), 237–244.
- Mortimer, N. 2004. New Zealand's geological foundations. *Gondwana Research*, **7** (1), 261–272.
- Mortimer, N. & Cooper, A.F. 2004. U-Pb and Sm-Nd ages from the Alpine Schist, New Zealand. *New Zealand Journal of Geology and Geophysics*, **47** (1), 21–28.

- Mortimer, N. & Parkinson, D. 1996. Hikurangi Plateau: a Cretaceous large igneous province in the southwest Pacific Ocean. *Journal of Geophysical Research*, **101** (B1), 687–696.
- Mortimer, N., Tulloch, A.J., Spark, R.N., Walker, N.W., Ladley, E., Allibone, A. & Kimbrough, D.L. 1999. Overview of the Median batholith, New Zealand: a new interpretation of the geology of the Median Tectonic Zone and adjacent rocks. *Journal of African Earth Sciences*, **29** (1), 257–268.
- Muir, R.J., Ireland, T.R., Weaver, S.D., Bradshaw, J.D., Evans, J.A., Eby, G.N. & Shelley, D. 1998. Geochronology and geochemistry of a Mesozoic magmatic arc system, Fiordland, New Zealand. *Journal of the Geological Society, London*, **155**, 1037–1052.
- Muir, R.J., Ireland, T.R., Weaver, S.D., Bradshaw, J.D., Waight, T.E., Jongens, R. & Eby, G.N. 1997. SHRIMP U-Pb geochronology of Cretaceous magmatism in northwest Nelson–Westland, South Island, New Zealand. *New Zealand Journal of Geology and Geophysics*, **40** (4), 453–463.
- Muller, R.A. 2002. Avalanches at the core-mantle boundary. *Geophysical Research Letters*, **29** (19), 1–4, 1935, 10.1029/2002GL015938.
- Muttoni, G., Kent, D.V., Garzanti, E., Brack, P., Abrahamsen, N. & Gaetani, M. 2003. Early Permian Pangea 'B' to Late Permian Pangea 'A'. *Earth and Planetary Science Letters*, **215** (3-4), 379–394.
- Nagalingum, N.S., Drinnan, A.N., Lupia, R. & McLoughlin, S. 2002. Fern spore diversity and abundance in Australia during the Cretaceous. *Review of Palaeobotany and Palynology*, **119** (1-2), 69–92.
- Nakanishi, M., Tamaki, K. & Kobayashi, K. 1992. A new Mesozoic isochron chart of the northwestern Pacific Ocean: paleomagnetic and tectonic implications. *Geophysical Research Letters*, **19** (7), 693–696.
- Nakanishi, M. & Winterer, E.L. 1998. Tectonic history of the Pacific–Farallon–Phoenix triple junction from late Jurassic to early Cretaceous: an abandoned Mesozoic spreading system in the central Pacific basin. *Journal of Geophysical Research*, **103** (B6), 12453–12468.
- Newell, N.D. 1967. Revolutions in the history of life. *Geological Society of America Special Paper*, **89**, 63–91.
- Nichols, G.J. & Cantrill, D.J. 2002. Tectonic and climatic controls on a Mesozoic forearc basin succession, Alexander Island, Antarctica. *Geological Magazine*, **139** (3), 313–330.
- Noble, S.R., Aspden, J.A. & Jemielita, R. 1997. Northern Andean crustal evolution: New U-Pb geochronological constraints from Ecuador. *Geological Society of America Bulletin*, **109** (7), 789–798.
- Nomade, S., Pouclet, A. & Chen, Y. 2002. The French Guyana doleritic dykes: geochemical evidence of three populations and new data for the Jurassic Central Atlantic Magmatic Province. *Journal of Geodynamics*, **34** (5), 595–614.
- Norris, R.J. & Cooper, A.F. 2003. Very high strains recorded in mylonites along the Alpine Fault, New Zealand: implications for the deep structure of plate boundary faults. *Journal of Structural Geology*, **25** (12), 2141–2157.
- Norris, R.J., Koons, P.O. & Cooper, A.F. 1990. The obliquely convergent plate boundary in the South Island of New Zealand: implications for ancient collision zones. *Journal of Structural Geology*, **12** (5-6), 715–725.
- Nzoussi-Mbassani, P., Disnar, J.R. & Laggoun-Defarge, F. 2003. Organic matter characteristics of Cenomanian-Turonian source rocks: implications for

- petroleum and gas exploration onshore Senegal. *Marine and Petroleum Geology*, **20** (5), 411–427.
- Obaje, N.G. & Hamza, H. 2000. Liquid hydrocarbon source-rock potential of mid-Cretaceous coals and coal measures in the Middle Benue Trough of Nigeria. *International Journal of Earth Sciences*, **89** (1), 130–139.
- Okamoto, K., Shinjoe, H., Katayama, I., Terada, K., Sano, Y. & Johnson, S. 2004. SHRIMP U-Pb zircon dating of quartz-bearing eclogite from the Sanbagawa Belt, south-west Japan: implications for metamorphic evolution of subducted protolith. *Terra Nova*, **16** (2), 81–89.
- Okay, A.I., Monod, O. & Monie, P. 2002. Triassic blueschists and eclogites from northwest Turkey: vestiges of the Paleo-Tethyan subduction. *Lithos*, **64** (3–4), 155–178.
- O'Sullivan, P.B., Foster, D.A., Kohn, B.P. & Gleadow, A.J.W. 1996. Multiple postorogenic denudation events: an example from the eastern Lachlan fold belt, Australia. *Geology*, **24** (6), 563–566.
- O'Sullivan, P.B., Mitchell, M.M., O'Sullivan, A.J., Kohn, B.P. & Gleadow, A.J.W. 2000. Thermotectonic history of the Bassian Rise, Australia: implications for the breakup of eastern Gondwana along Australia's southeastern margins. *Earth and Planetary Science Letters*, **182** (1), 31–47.
- Otto, S.C. 1997. Mesozoic-Cenozoic history of deformation and petroleum systems in sedimentary basins of Central Asia: implications of collisions on the Eurasian margin. *Petroleum Geoscience*, **3** (4), 327–341.
- Palfy, J. & Smith, P.L. 2000. Synchrony between Early Jurassic extinction, oceanic anoxic event, and the Karoo–Ferrar flood basalt volcanism. *Geology*, **28** (8), 747–750.
- Pan, Y.X., Hill, M.J., Zhu, R.X. & Shaw, J. 2004. Further evidence for low intensity of the geomagnetic field during the early Cretaceous time: using the modified Shaw method and microwave technique. *Geophysical Journal International*, **157** (2), 553–564.
- Pancost, R.D., Crawford, N., Magness, S., Turner, A., Jenkyns, H.C. & Maxwell, J.R. 2004. Further evidence for the development of photic-zone euxinic conditions during Mesozoic oceanic anoxic events. *Journal of the Geological Society, London*, **161** (3), 353–364.
- Pankhurst, R.J., Millar, I.L., Grunow, A.M. & Storey, B.C. 1993. The Pre-Cenozoic magmatic history of the Thurston Island crustal block, West Antarctica. *Journal of Geophysical Research*, **98** (B7), 11835–11849.
- Pankhurst, R.J., Riley, T.R., Fanning, C.M. & Kelley, S.P. 2000. Episodic silicic volcanism in Patagonia and the Antarctic Peninsula: chronology of magmatism associated with the break-up of Gondwana. *Journal of Petrology*, **41** (5), 605–625.
- Pankhurst, R.J. & Rowley, P.D. 1991. Rb-Sr study of Cretaceous plutons from southern Antarctic Peninsula and eastern Ellsworth Land, Antarctica. In: Thomson, M.R.A., Crame, J.A. & Thomson, J.W. (eds) *Geological Evolution of Antarctica*. Cambridge University Press, Cambridge, 387–394.
- Pankhurst, R.J., Weaver, S.D., Herve, F. & Larrondo, P. 1999. Mesozoic–Cenozoic evolution of the North Patagonian batholith in Aysen, southern Chile. *Journal of the Geological Society, London*, **156** (4), 673–694.
- Parkinson, C.D., Miyazaki, K., Wakita, K., Barber, A.J. & Carswell, D.A. 1998. An overview and tectonic synthesis of the pre-Tertiary very- high-pressure

- metamorphic and associated rocks of Java, Sulawesi and Kalimantan, Indonesia. *Island Arc*, **7** (1-2), 184–200.
- Paull, C.K., Ussler, W. & Dillon, W.P. 1991. Is the extent of glaciation limited by marine gas hydrates? *Geophysical Research Letters*, **18** (3), 432–434.
- Pe-Piper, G. & Reynolds, P.H. 2000. Early Mesozoic alkaline mafic dykes, southwestern Nova Scotia, Canada, and their bearing on Triassic-Jurassic magmatism. *Canadian Mineralogist*, **38**, 217–232.
- Pindell, J.L. & Barrett, S. 1990. Geological evolution of the Caribbean region; a plate tectonic perspective. In: Dengo, G. & Case, J. (eds) *The Caribbean Region, The Geology of North America*. Colorado Geological Society, Boulder, **Vol. H**, 405–432.
- Plasienka, D. 2003. Development of basement-involved fold and thrust structures exemplified by the Tatric-Fatric-Veporic nappe system of the Western Carpathians (Slovakia). *Geodynamica Acta*, **16** (1), 21–38.
- Prokoph, A., Ernst, R.E. & Buchan, K.L. 2004. Time-series analysis of large igneous provinces: 3500 Ma to present. *Journal of Geology*, **112** (1), 1–22.
- Qi, J.Z., Yuan, S.S., Liu, Z.J., Liu, D.Y., Wang, Y.B., Li, Z.H., Guo, J.H. & Sun, B. 2004. U-Pb SHRIMP dating of zircon from quartz veins of the Yangshan gold deposit in Gansu Province and its geological significance. *Acta Geologica Sinica-English Edition*, **78** (2), 443–451.
- Quinn, M.J., Wright, J.E. & Wyld, S.J. 1997. Happy Creek igneous complex and tectonic evolution of the early Mesozoic arc in the Jackson Mountains, northwest Nevada. *Geological Society of America Bulletin*, **109** (4), 461–482.
- Rapela, C.W., Pankhurst, R.J. & Harrison, S.M. 1992. Triassic Gondwana granites of the Gastre district, North Patagonian massif. *Transactions of the Royal Society of Edinburgh-Earth Sciences*, **83**, 291–304.
- Retallack, G.J. 2002. Carbon dioxide and climate over the past 300 Myr. *Philosophical Transactions of the Royal Society of London Series A*, **360** (1793), 659–673.
- Ricou, L.E. 1994. Tethys reconstructed: plates, continental fragments and their boundaries since 260-Ma from Central America to south-eastern Asia. *Geodynamica Acta*, **7** (4), 169–218.
- Riding, J.B. & Crame, J.A. 2002. Aptian to Coniacian (Early-Late Cretaceous) palynostratigraphy of the Gustav Group, James Ross Basin, Antarctica. *Cretaceous Research*, **23**, 739–760.
- Riley, T.R. & Knight, K.B. 2001. Age of pre-break-up Gondwana magmatism. *Antarctic Science*, **13** (2), 99–110.
- Riley, T.R., Leat, P.T., Pankhurst, R.J. & Harris, C. 2001. Origins of large volume rhyolitic volcanism in the Antarctic Peninsula and Patagonia by crustal melting. *Journal of Petrology*, **42** (6), 1043–1065.
- Riley, T.R., Millar, I.L., Watkeys, M.K., Curtis, M.L., Leat, P.T., Klausen, M.B. & Fanning, C.M. 2004. U-Pb zircon (SHRIMP) ages for the Lebombo rhyolites, South Africa: refining the duration of Karoo volcanism. *Journal of the Geological Society, London*, **161** (2), 547–550.
- Roger, F., Malavieille, J., Leloup, P.H., Calassou, S. & Xu, Z. 2004. Timing of granite emplacement and cooling in the Songpan-Garze Fold Belt (eastern Tibetan Plateau) with tectonic implications. *Journal of Asian Earth Sciences*, **22** (5), 465–481.
- Roland, N.W. & Tessensohn, F. 1987. Rennick faulting: an early phase of Ross Sea rifting. *Geologisches Jahrbuch*, **B66**, 203–229.

- Rossetti, F., Lisker, F., Storti, F. & Laufer, A.L. 2003. Tectonic and denudational history of the Rennick Graben (North Victoria Land): Implications for the evolution of rifting between East and West Antarctica. *Tectonics*, **22** (2), 1–22, 1016, 10.1029/2002TC001416.
- Ruffell, A. 1995. Evolution and hydrocarbon prospectivity of the Brittany Basin (Western Approaches Trough), offshore north-west France. *Marine and Petroleum Geology*, **12** (4), 387–407.
- Sakashima, T., Terada, K., Takeshita, T. & Sano, Y. 2003. Large-scale displacement along the Median Tectonic Line, Japan: evidence from SHRIMP zircon U-Pb dating of granites and gneisses from the South Kitakami and paleo-Ryoke belts. *Journal of Asian Earth Sciences*, **21** (9), 1019–1039.
- Sato, K., Vrublevisky, A.A., Rodionov, S.M., Romanovsky, N.P. & Nedachi, M. 2002. Mid-Cretaceous episodic magmatism and tin mineralization in Khingan-Okhotsk volcano-plutonic belt, Far East Russia. *Resource Geology*, **52** (1), 1–14.
- Schermer, E.R., Stephens, K.A. & Walker, J.D. 2001. Paleogeographic and tectonic implications of the geology of the Tiefert Mountains, northern Mojave Desert, California. *Geological Society of America Bulletin*, **113** (7), 920–938.
- Scheuber, E. & Gonzalez, G. 1999. Tectonics of the Jurassic- Early Cretaceous magmatic arc of the north Chilean Coastal Cordillera (22° S–26° S): a story of crustal deformation along a convergent plate boundary. *Tectonics*, **18** (5), 895–910.
- Schouten, S., Van Kaam-Peters, H.M.E., Rijpstra, W.I.C., Schoell, M. & Damste, J.S.S. 2000. Effects of an oceanic anoxic event on the stable carbon isotopic composition of Early Toarcian carbon. *American Journal of Science*, **300** (1), 1–22.
- Sephton, M.A., Amor, K., Franchi, I.A., Wignall, P.B., Newton, R. & Zonneveld, J.P. 2002. Carbon and nitrogen isotope disturbances and an end-Norian (Late Triassic) extinction event. *Geology*, **30** (12), 1119–1122.
- Siddoway, C.S., Baldwin, S.L., Fitzgerald, P.G., Fanning, C.M. & Luyendyk, B.P. 2004. Ross Sea mylonites and the timing of intracontinental extension within the West Antarctic rift system. *Geology*, **32** (1), 57–60.
- Siddoway, C.S., Sass III, L.C. & Esser, R.P. in press. Kinematic history of the Marie Byrd Land terrane, West Antarctica: Direct evidence from Cretaceous mafic dykes. In: Vaughan, A.P.M., Leat, P.T. & Pankhurst, R.J. (eds) *Terrane processes at the margin of Gondwana*. Geological Society, London, Special Publications, this volume.
- Silva-Romo, G., Arellano-Gil, J., Mendoza-Rosales, C. & Nieto-Obregon, J. 2000. A submarine fan in the Mesa Central, Mexico. *Journal of South American Earth Sciences*, **13** (4-5), 429–442.
- Smellie, J.L. 1981. A complete arc–trench system recognized in Gondwana sequences of the Antarctic Peninsula region. *Geological Magazine*, **118** (2), 139–159.
- Smellie, J.L., Roberts, B. & Hiron, S.R. 1996. Very low- and low-grade metamorphism in the Trinity Peninsula Group (Permo-Triassic) of northern Graham Land, Antarctic Peninsula. *Geological Magazine*, **133** (5), 583–594.
- Smith, C.A., Sisson, V.B., Lallemand, H.G.A. & Copeland, P. 1999. Two contrasting pressure-temperature-time paths in the Villa de Cura blueschist belt, Venezuela: possible evidence for Late Cretaceous initiation of subduction in the Caribbean. *Geological Society of America Bulletin*, **111** (6), 831–848.

- Solheim, L.P. & Peltier, W.R. 1994. Avalanche effects in phase transition modulated thermal convection: a model of Earth's mantle. *Journal of Geophysical Research*, **99** (B4), 6997–7018.
- Spell, T.L., McDougall, I. & Tulloch, A.J. 2000. Thermochronologic constraints on the breakup of the Pacific Gondwana margin: The Paparoa metamorphic core complex, South Island, New Zealand. *Tectonics*, **19** (3), 433–451.
- Sporli, K.B. 1978. Mesozoic tectonics, North Island, New Zealand. *Geological Society of America Bulletin*, **89**, 415–425.
- Stavsky, A.P., Chekhovitch, V.D., Kononov, M.V. & Zonenshain, L.P. 1990. Plate tectonics and palinspastic reconstructions of the Anadyr- Koryak Region, northeast USSR. *Tectonics*, **9** (1), 81–101.
- Stein, G., Lapiere, H., Monod, O., Zimmermann, J.L. & Vidal, R. 1994. Petrology of some Mexican Mesozoic–Cenozoic plutons: sources and tectonic environments. *Journal of South American Earth Sciences*, **7** (1), 1–7.
- Stevens, R.A. & Erdmer, P. 1996. Structural divergence and transpression in the Teslin tectonic zone, southern Yukon Territory. *Tectonics*, **15** (6), 1342–1363.
- Storey, B.C. 1995. The role of mantle plumes in continental breakup: case histories from Gondwanaland. *Nature*, **377** (6547), 301–308.
- Storey, B.C., Brown, R.W., Carter, A., Doubleday, P.A., Hurford, A.J., Macdonald, D.I.M. & Nell, P.A.R. 1996. Fission-track evidence for the thermotectonic evolution of a Mesozoic–Cenozoic fore-arc, Antarctica. *Journal of the Geological Society, London*, **153** (1), 65–82.
- Storey, B.C., Hole, M.J., Pankhurst, R.J., Millar, I.L. & Vennum, W. 1988. Middle Jurassic within-plate granites in West Antarctica and their bearing on the break-up of Gondwanaland. *Journal of the Geological Society, London*, **145** (6), 999–1007.
- Storey, B.C. & Kyle, P.R. 1997. An active mantle mechanism for Gondwana breakup. *South African Journal of Geology*, **100** (4), 283–290.
- Storey, B.C., Thomson, M.R.A. & Meneilly, A.W. 1987. The Gondwanian Orogeny within the Antarctic Peninsula: a discussion. In: McKenzie, G.D. (ed.) *Gondwana Six: Structure, Tectonics and Geophysics*. Geophysical Monograph Series. American Geophysical Union, Washington D.C., **41**, 191–197.
- Stovba, S.M. & Stephenson, R.A. 1999. The Donbas Foldbelt: its relationships with the uninverted Donets segment of the Dniepr-Donets Basin, Ukraine. *Tectonophysics*, **313** (1-2), 59–83.
- Strasser, A., Caron, M. & Gjermeni, M. 2001. The Aptian, Albian and Cenomanian of Roter Sattel, Romandes Prealps, Switzerland: a high-resolution record of oceanographic changes. *Cretaceous Research*, **22** (2), 173–199.
- Sutherland, R., Davey, F. & Beavan, J. 2000. Plate boundary deformation in South Island, New Zealand, is related to inherited lithospheric structure. *Earth and Planetary Science Letters*, **177** (3-4), 141–151.
- Sutherland, R. & Hollis, C. 2001. Cretaceous demise of the Moa plate and strike-slip motion at the Gondwana margin. *Geology*, **29** (3), 279–282.
- Tackley, P.J., Stevenson, D.J., Glatzmaier, G.A. & Schubert, G. 1994. Effects of multiple phase-transitions in a 3-dimensional spherical model of convection in Earth's mantle. *Journal of Geophysical Research*, **99** (B8), 15877–15901.
- Tanner, L.H., Lucas, S.G. & Chapman, M.G. 2004. Assessing the record and causes of Late Triassic extinctions. *Earth-Science Reviews*, **65** (1-2), 103–139.

- Tarduno, J.A., Cottrell, R.D. & Smirnov, A.V. 2001. High geomagnetic intensity during the mid-Cretaceous from Thellier analyses of single plagioclase crystals. *Science*, **291** (5509), 1779-1783.
- Tarduno, J.A., Cottrell, R.D. & Smirnov, A.V. 2002. The Cretaceous superchron geodynamo: Observations near the tangent cylinder. *Proceedings of the National Academy of Sciences of the United States of America*, **99** (22), 14020-14025.
- Tardy, M., Lapierre, H., Freydier, C., Coulon, C., Gill, J.B., Delepinay, B.M., Beck, C., Martinez, J., Talavera, O., Ortiz, E., Stein, G., Bourdier, J.L. & Yta, M. 1994. The Guerrero suspect terrane (western Mexico) and coeval arc terranes (the Greater Antilles and the Western Cordillera of Colombia): a Late Mesozoic intraoceanic arc accreted to cratonal America during the Cretaceous. *Tectonophysics*, **230** (1-2), 49-73.
- Tate, M.C. & Johnson, S.E. 2000. Subvolcanic and deep-crustal tonalite genesis beneath the Mexican peninsular ranges. *Journal of Geology*, **108** (6), 721-728.
- Tessensohn, F. 1994. The Ross Sea region: structural interpretation in relation to the evolution of the Southern Ocean. *Terra Antartica*, **1** (3), 553-558.
- Thiele, R. & Pincheira, M. 1987. Tectonica transpresiva y movimiento de desgarre en el segmento sur de la Zona de la Falla Atacama, Chile. *Revista Geológica de Chile*, **31**, 77-94.
- Thomas, J.C., Cobbold, P.R., Shein, V.S. & Le Douaran, S. 1999. Sedimentary record of late Paleozoic to Recent tectonism in central Asia - analysis of subsurface data from the Turan and south Kazak domains. *Tectonophysics*, **313** (3), 243-263.
- Thomson, B., Aftalion, M., McIntyre, R.M. & Rice, C. 1995. Geochronology and tectonic setting of silicic dike swarms and related silver mineralization at Candelaria, western Nevada. *Economic Geology and the Bulletin of the Society of Economic Geologists*, **90** (8), 2182-2196.
- Thomson, C.N. & Girty, G.H. 1994. Early Cretaceous intra-arc ductile strain in Triassic-Jurassic and Cretaceous continental-margin arc rocks, Peninsular Ranges, California. *Tectonics*, **13** (5), 1108-1119.
- Thomson, M.R.A. & Tranter, T.H. 1986. Early Jurassic fossils from central Alexander Island and their geological setting. *British Antarctic Survey Bulletin*, **No. 70**, 23-39.
- Thomson, S.N. & Herve, F. 2002. New time constraints for the age of metamorphism at the ancestral Pacific Gondwana margin of southern Chile (42° S-52° S). *Revista Geológica de Chile*, **29** (2), 255-271.
- Till, A.B., Box, S.E., Roeske, S.M. & Patton, W.W. 1993. Mid-Cretaceous extensional fragmentation of a Jurassic-Early Cretaceous compressional orogen, Alaska - Comment. *Tectonics*, **12** (4), 1076-1081.
- Till, A.B. & Snee, L.W. 1995. ⁴⁰Ar/³⁹Ar evidence that formation of blueschists in continental-crust was synchronous with foreland fold-and-thrust belt deformation, western Brooks Range, Alaska. *Journal of Metamorphic Geology*, **13** (1), 41-60.
- Toro, J., Amato, J.M. & Natal'in, B. 2003. Cretaceous deformation, Chegitun River area, Chukotka Peninsula, Russia: implications for the tectonic evolution of the Bering Strait region. *Tectonics*, **22** (3), 1-17, 1021, 10.1029/2001TC001333.

- Torsvik, T.H. & Andersen, T.B. 2002. The Taimyr fold belt, Arctic Siberia: timing of prefold remagnetisation and regional tectonics. *Tectonophysics*, **352** (3-4), 335–348.
- Tranter, T.H. 1987. The structural history of the LeMay Group of central Alexander Island, Antarctic Peninsula. *British Antarctic Survey Bulletin*, **No. 77**, 61–80.
- Trouw, R.A.J., Passchier, C.W., Simoes, L.S.A., Andreis, R.R. & Valeriano, C.M. 1997. Mesozoic tectonic evolution of the South Orkney microcontinent, Scotia arc, Antarctica. *Geological Magazine*, **134** (3), 383–401.
- Trouw, R.A.J., Passchier, C.W., Valeriano, C.M., Simoes, L.S.A., Paciullo, F.V.P. & Ribeiro, A. 2000. Deformational evolution of a Cretaceous subduction complex: Elephant Island, South Shetland Islands, Antarctica. *Tectonophysics*, **319** (2), 93–110.
- Tulloch, A.J., Kimbrough, D.L., Landis, C.A., Mortimer, N. & Johnston, M.R. 1999. Relationships between the Brook Street terrane and Median Tectonic Zone (Median batholith): evidence from Jurassic conglomerates. *New Zealand Journal of Geology and Geophysics*, **42** (2), 279–293.
- Ueda, H., Kawamura, M. & Niida, K. 2000. Accretion and tectonic erosion processes revealed by the mode of occurrence and geochemistry of greenstones in the Cretaceous accretionary complexes of the Idonnappu Zone, southern central Hokkaido, Japan. *Island Arc*, **9** (2), 237–257.
- Umhoefer, P.J. & Miller, R.B. 1996. Mid-Cretaceous thrusting in the southern Coast Belt, British Columbia and Washington, after strike-slip fault reconstruction. *Tectonics*, **15** (3), 545–565.
- Vaughan, A.P.M. 1995. Circum-Pacific mid-Cretaceous deformation and uplift - a superplume-related event? *Geology*, **23** (6), 491–494.
- Vaughan, A.P.M., Kelley, S.P. & Storey, B.C. 2002a. Mid-Cretaceous ductile deformation on the Eastern Palmer Land Shear Zone, Antarctica, and implications for timing of Mesozoic terrane collision. *Geological Magazine*, **139** (4), 465–471.
- Vaughan, A.P.M., Millar, I.L. & Thistlewood, L. 1999. The Auriga Nunataks shear zone: Mesozoic transfer faulting and arc deformation in northwest Palmer Land, Antarctica. *Tectonics*, **18** (5), 911–928.
- Vaughan, A.P.M., Pankhurst, R.J. & Fanning, C.M. 2002b. A mid-Cretaceous age for the Palmer Land event, Antarctic Peninsula: implications for terrane accretion timing and Gondwana palaeolatitudes. *Journal of the Geological Society, London*, **159** (2), 113–116.
- Vaughan, A.P.M. & Scarrow, J.H. 2003. Ophiolite obduction pulses as a proxy indicator of superplume events? *Earth and Planetary Science Letters*, **213** (3-4), 407–416.
- Vaughan, A.P.M. & Storey, B.C. 2000. The eastern Palmer Land shear zone: a new terrane accretion model for the Mesozoic development of the Antarctic Peninsula. *Journal of the Geological Society, London*, **157** (6), 1243–1256.
- Vermeij, G.J. 1995. Economics, volcanoes, and Phanerozoic revolutions. *Paleobiology*, **21** (2), 125–152.
- Vielreicher, R.M., Vielreicher, N.M., Hagemann, S.G. & Jones, G. 2003. Fault zone evolution and its controls on ore-grade distribution at the Jian Cha Ling gold deposit, western Qinling region, central China. *Mineralium Deposita*, **38** (5), 538–554.
- Vry, J.K., Baker, J., Maas, R., Little, T.A., Grapes, R. & Dixon, M. 2004. Zoned (Cretaceous and Cenozoic) garnet and the timing of high grade

- metamorphism, Southern Alps, New Zealand. *Journal of Metamorphic Geology*, **22** (3), 137–157.
- Waight, T.E., Weaver, S.D. & Muir, R.J. 1998. Mid-Cretaceous granitic magmatism during the transition from subduction to extension in southern New Zealand: a chemical and tectonic synthesis. *Lithos*, **45** (1-4), 469–482.
- Wang, Z.H. 2002. The origin of the Cretaceous gabbros in the Fujian coastal region of SE China: implications for deformation-accompanied magmatism. *Contributions to Mineralogy and Petrology*, **144** (2), 230–240.
- Wang, Z.H. & Lu, H.F. 1997. $^{40}\text{Ar}/^{39}\text{Ar}$ geochronology and exhumation of mylonitized metamorphic complex in Changle-Nanao ductile shear zone. *Science in China, Series D-Earth Sciences*, **40** (6), 641–647.
- Wang, Z.H. & Lu, H.F. 1998. Geology, petrology and geochemistry of the mafic-ultramafic rocks in the Fujian coastal region, southeastern China, and their genesis. *Ophioliti*, **23** (1), 1–6.
- Weiland, T.J., Suayah, I.B. & Finch, R.C. 1992. Petrologic, stratigraphic and tectonic significance of Mesozoic volcanic-rocks in the Rio-Wampu area, Eastern Honduras. *Journal of South American Earth Sciences*, **6** (4), 309–325.
- Wever, H.E., Storey, B.C. & Leat, P. 1995. Peraluminous granites in NE Palmer Land, Antarctic Peninsula: early Mesozoic crustal melting in a magmatic arc. *Journal of the Geological Society, London*, **152** (1), 85–96.
- Wignall, P.B. 2001. Large igneous provinces and mass extinctions. *Earth-Science Reviews*, **53** (1-2), 1–33.
- Wilson, P.A., Jenkyns, H.C., Elderfield, H. & Larson, R.L. 1998. The paradox of drowned carbonate platforms and the origin of Cretaceous Pacific guyots. *Nature*, **392** (6679), 889–894.
- Wilson, P.A. & Norris, R.D. 2001. Warm tropical ocean surface and global anoxia during the mid-Cretaceous period. *Nature*, **412** (6845), 425–429.
- Windley, B.F. 1995. *The Evolving Continents*. Wiley, Chichester.
- Wyld, S.J., Rogers, J.W. & Wright, J.E. 2001. Structural evolution within the Luning-Fencemaker fold-thrust belt, Nevada: progression from back-arc basin closure to intra- arc shortening. *Journal of Structural Geology*, **23** (12), 1971–1995.
- Xiao, W.J., Windley, B.F., Chen, H.L., Zhang, G.C. & Li, J.L. 2002. Carboniferous-Triassic subduction and accretion in the western Kunlun, China: Implications for the collisional and accretionary tectonics of the northern Tibetan Plateau. *Geology*, **30** (4), 295–298.
- Yang, Z.Y., Moreau, M.G., Bucher, H., Dommergues, J.L. & Trouiller, A. 1996. Hettangian and Sinemurian magnetostratigraphy from Paris Basin. *Journal of Geophysical Research-Solid Earth*, **101** (B4), 8025–8042.
- Yong, L., Allen, P.A., Densmore, A.L. & Qiang, X. 2003. Evolution of the Longmen Shan Foreland Basin (Western Sichuan, China) during the Late Triassic Indosinian orogeny. *Basin Research*, **15** (1), 117–138.
- Zagorcev, I.S. 1994. Structure and tectonic evolution of the Pirin-Pangaion structural zone (Rhodope Massif, southern Bulgaria and northern Greece). *Geological Journal*, **29** (3), 241–268.
- Zhang, X.H., Li, T.S. & Pu, Z.P. 2002. $^{40}\text{Ar}/^{39}\text{Ar}$ thermochronology of two ductile shear zones from Yiwulushan, West Liaoning Region: age constraints on the Mesozoic tectonic events. *Chinese Science Bulletin*, **47** (13), 1113–1118.
- Ziabrev, S.V., Aitchison, J.C., Abrajevitch, A.V., Badengzhu, Davis, A.M. & Luo, H. 2004. Bainang Terrane, Yarlung-Tsangpo suture, southern Tibet (Xizang, China): a record of intra-Neotethyan subduction- accretion processes

preserved on the roof of the world. *Journal of the Geological Society, London*, **161** (3), 523–538.

Figure Captions

Figure 1: Distribution of areas preserving Late Triassic-Early Jurassic deformation and magmatism on 200 Ma reconstruction of the Pangaea supercontinent. Areas of large igneous provinces or inferred oceanic plateaus outlined with dashed line; kimberlite magmatism marked with *K*; plutonism marked with a star. AI Alexander Island, *CAMP* Central Atlantic Magmatic Province, CC Coastal Cordillera, CI Central Iran, C/M Chonos/Madre de Dios accretionary complexes, CT Cache Creek Terrane, *CTP* Cache Creek Terrane plateau, DF Donbas fold belt, FP Fujian Province, GB Gobi Basin, GF Gastre fault system, *GLIP* Gondwana Large Igneous Province, IA Izmir–Ankara suture, KM Kunlun Mountains, LI Liaoning Province, MC Mesa Central, MH McHugh Complex, NN north-central Nevada, NS North China–South China block collision zone, *NUP* Nilüfer Unit plateau, NO Novaya Zemlya, OT Oaxaca Terrane, PE Peninsular Malaysia, PM Pensacola Mountains, QT Quesnel Terrane, SC Scotia Complex, SD Song-Da zone, SG Songpan-Garz, TA Taimyr Peninsula, TP Trinity Peninsula, TZ Teslin tectonic zone, WN western Nevada, YT Yukon-Tanana Terrane.

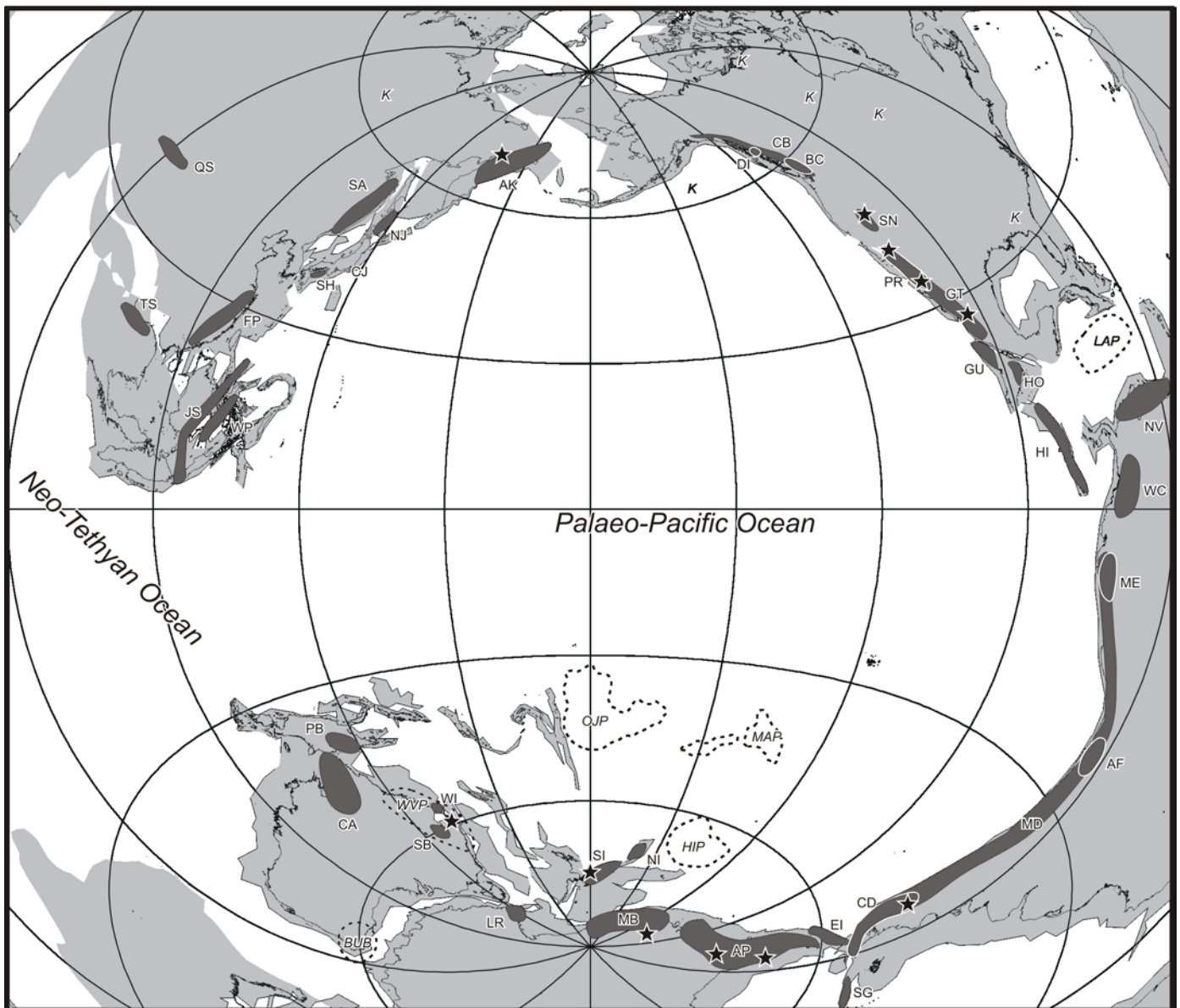
Figure 2: Distribution of areas preserving mid-Cretaceous deformation and magmatism on 100 Ma reconstruction of the Pacific basin. Areas of large igneous provinces or inferred oceanic plateaus outlined with dashed line; kimberlite magmatism marked with *K*; plutonism marked with a star. AF Atacama Fault, AK Anadyr-Koryak region, AP Antarctic Peninsula, BC British Columbia, *BUB* Bunbury Basalts, CA Carpentaria Basin, CB Coast Belt, CD Cordillera Darwin, CJ central Japan, DI Duke Island, EI Elephant Island, FP Fujian Province, GU Guatemala, HI Hispaniola, *HIP* Hikurangi plateau, HO Honduras, JS Java-Kalimantan-Sulawesi, *LAP* Lesser Antilles plateau, LR Lanterman Range, *MAP* Manihiki plateau, MB Marie Byrd Land, MD Mirano Diastrophic Phase, ME Mochica Event, NI North Island, New Zealand, NJ northern Japan, NV northern Venezuela, *OJP* Ontong-Java Plateau, PB Papuan Basin, QS Qilian Shan, SA Sikhote-Alin Mountains, SB Surat Basin, SG South Georgia, SH Shikoku SN Sierra Nevada, SI South Island, New Zealand, TS Truong-Son Belt, WC western Columbia, WI Whitsunday Islands, WP Western Philippines, *WVP* Whitsunday Volcanic Province and associated magmatism.

Figure 3: Plot of likely superplume-related events for the Phanerozoic (modified from Vaughan & Scarrow (2003)). Cumulative frequency plot of ophiolite age data from Vaughan & Scarrow (2003). Significant Phanerozoic geomagnetic events from Algeo (1996) and modified Phanerozoic sea level curve from Algeo (1996) and Algeo & Sclavinsky (1995). Major tectonic events from Vaughan (1995) and Windley (1995), and pre-Mesozoic proxy data from Doblas *et al.* (1998), Lehmann *et al.* (1995), Hennessy & Mossman (1996) and Connolly & Miller (2002). Data and age ranges for Mid-Cretaceous and Palaeozoic superplume events shown (Larson 1991a, b). Asterisks mark major changes in plate velocity discussed in text.

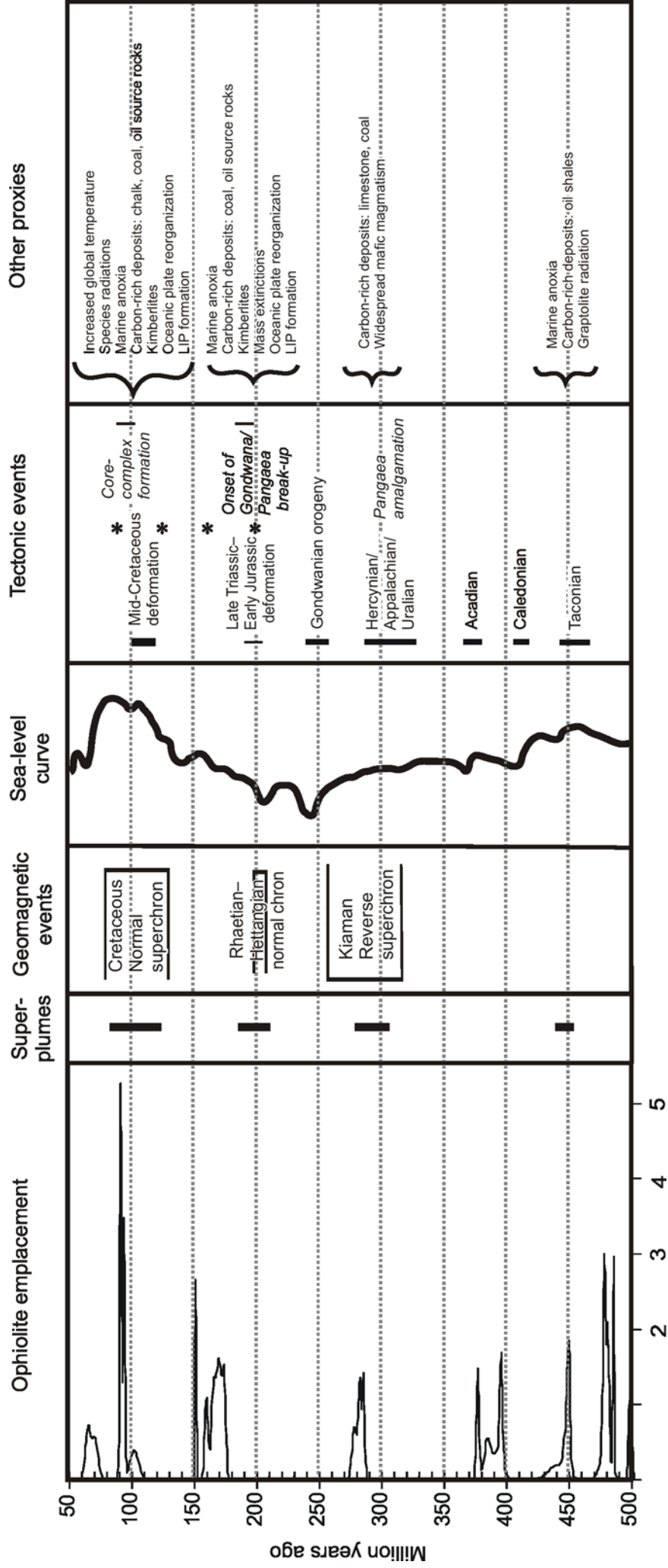
Figure 4: a) non-superplume state for notional section through the earth with large ocean and marginal basin ("oceanic" case); b) superplume state with active rising plumes from the D" layer.

Figure 5: a) non-superplume state for notional section through the earth with large supercontinent ("continental" case); b) superplume state with active rising plumes from the D" layer and onset of supercontinental break-up.

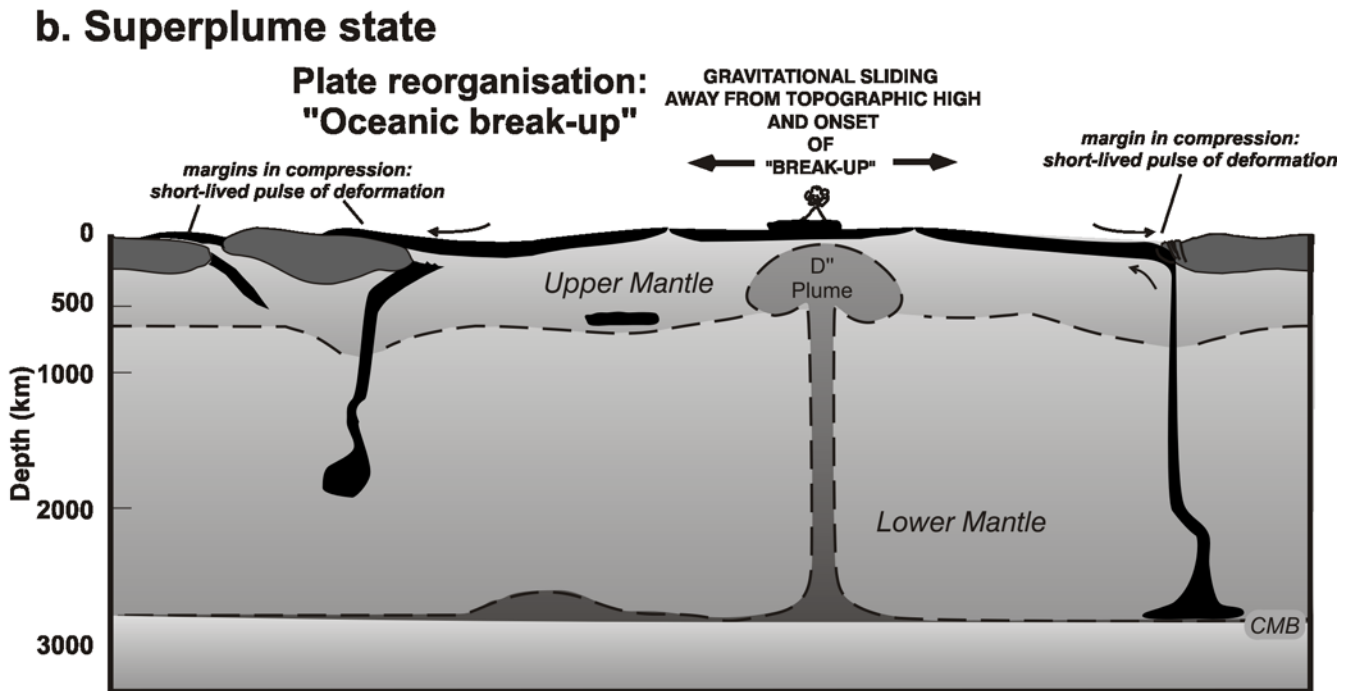
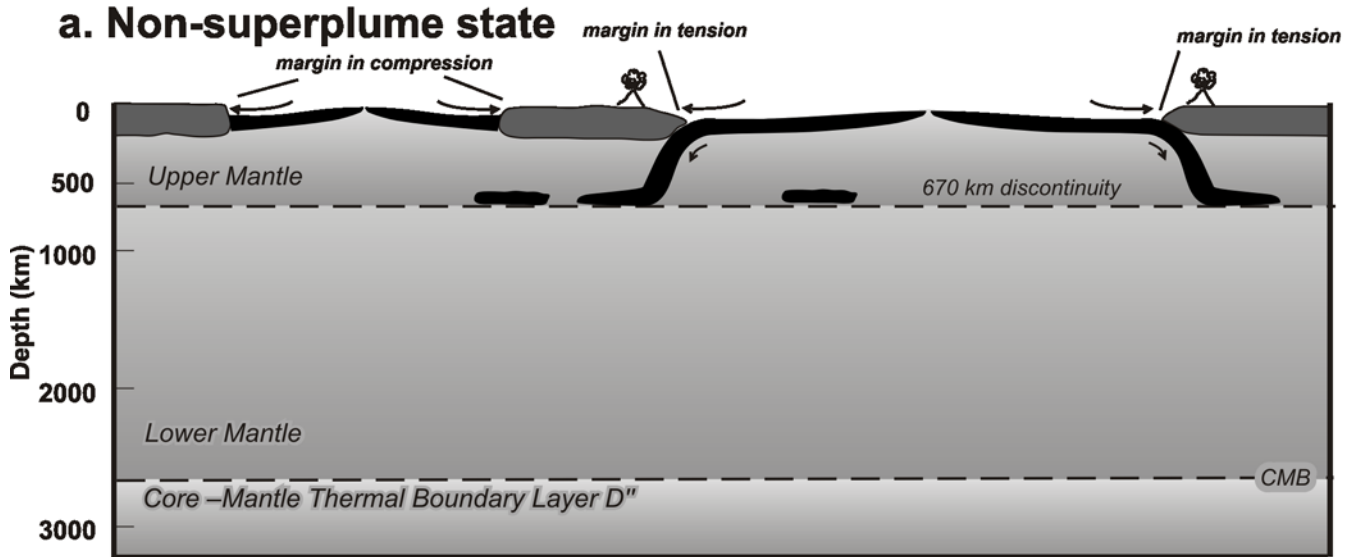
Vaughan & Livermore Fig. 2



Vaughan & Livermore Fig. 3

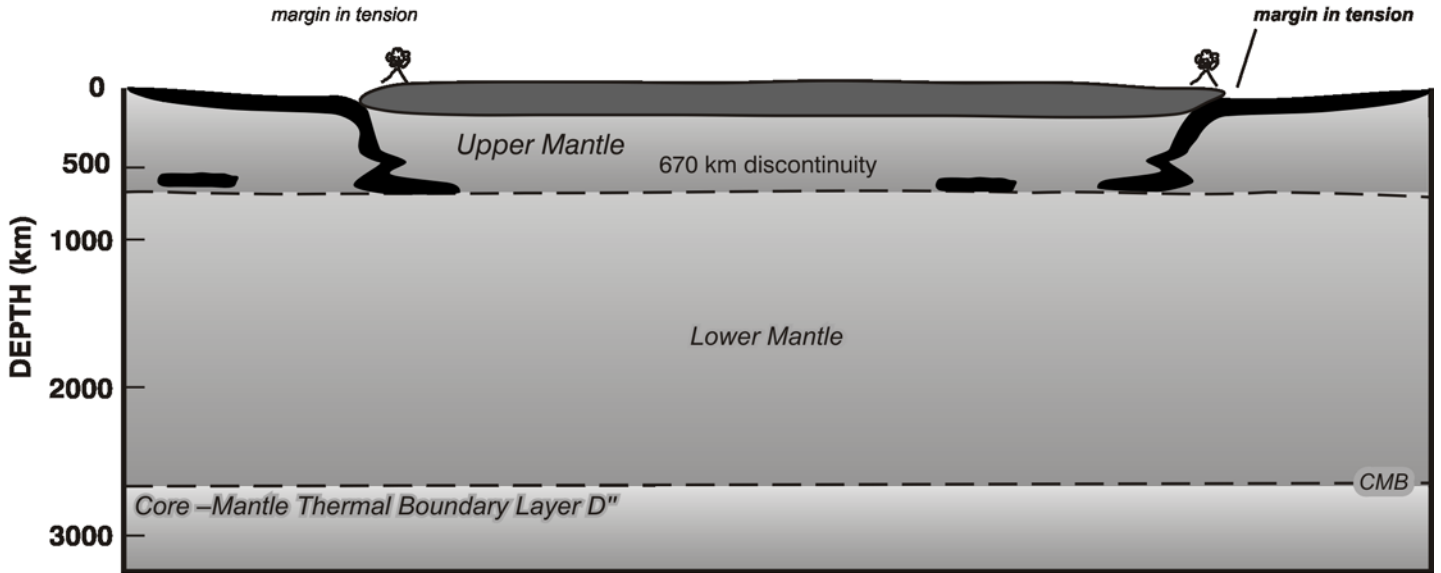


Vaughan & Livermore Fig. 4



Vaughan & Livermore Fig. 5

a. Non-superplume state



b. Superplume state

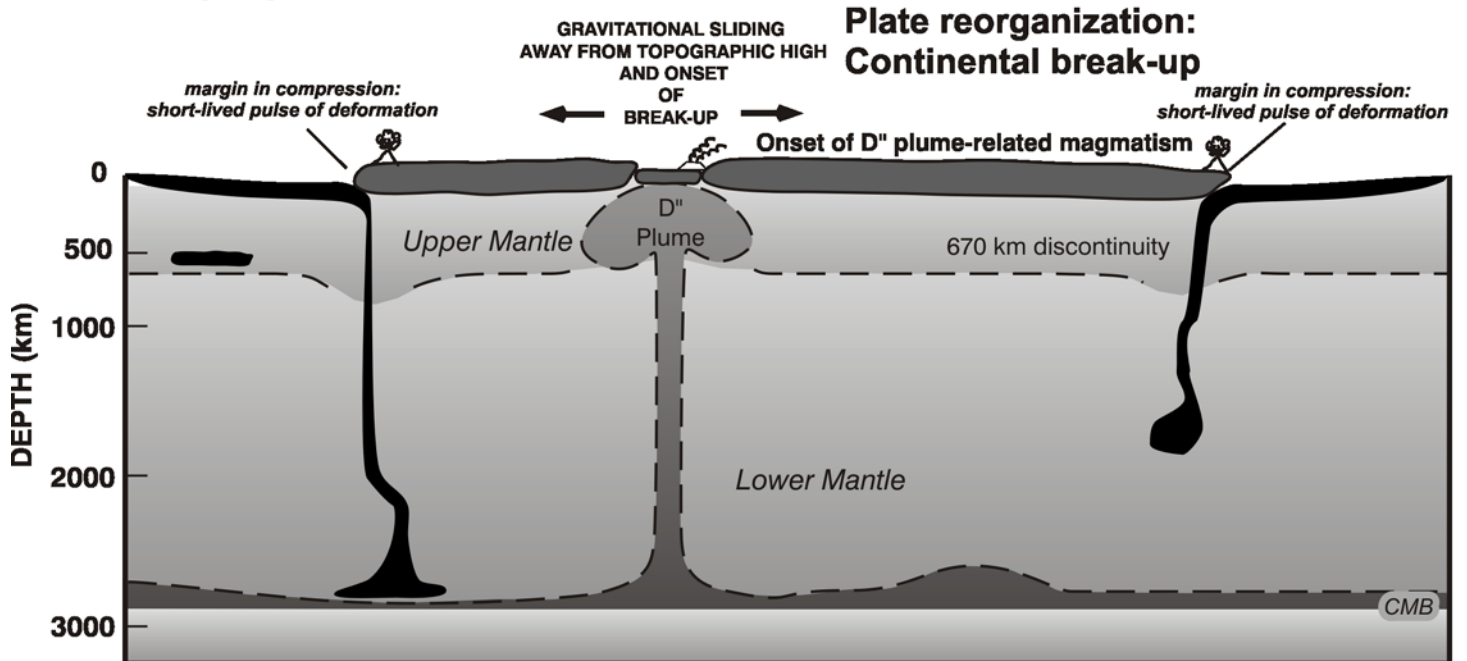


Table 1: Triassic–Jurassic events

Location	Event	Timing	Dating technique/criteria
<i>Antarctica</i>			
South Orkney Islands	Deformation and metamorphism of Scotia complex rocks	Post-Triassic and pre-Early to Middle Jurassic (200–176 Ma)	Interval between youngest deformed rocks and oldest unconformable sediments
Antarctic Peninsula	Peninsula Orogeny affecting Alexander Island and Trinity Peninsula accretionary rocks	Post-Triassic and pre-Middle Jurassic	Interval between youngest deformed rocks and oldest unconformable sediments
Pensacola Mountains	D ₃ phase of deformation in Patuxent Range	Post Early Triassic and pre-183 Ma	Interval between end of Permo-Triassic Gondwanian deformation and intrusion of lamprophyre dyke.
<i>South America</i>			
Patagonia	Deformation and metamorphism of Madre de Dios and Chonos accretionary complex rocks	234–198 Ma	Combined zircon fission track and U-Pb method dating.
North Chilean Coastal Cordillera	Transpressional deformation of Bolfin Complex amphibolites	200–174 Ma	U-Pb zircon method dating of syn-deformational igneous protoliths (200–191 Ma) and post deformational granite (174 Ma)
<i>Central and North America</i>			
SW Mexico	Thrusting and folding of sedimentary rocks, Oaxaca Terrane	post-early Permian and pre-Middle Jurassic	Interval between youngest deformed rocks and oldest unconformable sediments, and geometric correlation of structures
Mesa Central, Mexico	Thrusting of submarine fan deposits, Guerrero and Sierra Madre terranes	Post Norian and pre-Aalenian (203–175 Ma)	Interval between youngest deformed rocks and oldest unconformable sediments
Nevada, USA	Overthrusting of marine clastic rocks by ophiolitic melange	Post-mid-Triassic and pre-Late Triassic–Early Jurassic	Interval between youngest deformed rocks and post-deformational felsic dykes (222–192 Ma)
Nevada, USA	Activity on Luning–Fencemaker Thrust Belt	201–193 Ma	Ar-Ar dating of deformation structures
Canadian Cordillera	Imbrication of Cache Creek Terrane	210–173 Ma	Interval between eruption of basaltic lavas (210 Ma) and intrusion of cross-cutting pluton (173 Ma)
SE British Columbia	Deformation of Quesnel Terrane	215–197 Ma	Interval between intrusion of subsequently deformed diorite (215 Ma) and intrusion of cross-cutting plutons (197–181 Ma)
E Central Alaska	Imbrication of arc, subduction complex and continental rocks	Late Triassic to Early Jurassic (212–188 Ma)	Interval between intrusion of subsequently deformed granite (212 Ma) and Ar-Ar cooling ages in sheared rocks (188–185 Ma)
Southern Yukon Territory	Yukon-Tanana terrane ductile thrust deformation	Late Triassic to Early Jurassic	Interval between youngest deformed rocks and oldest unconformable sediments
SE Alaska	Blueschist metamorphism of McHugh Complex	~195 Ma	Ar-Ar dating of deformation structures
<i>Eurasia</i>			
Taimyr Peninsula	Strike-slip and folding of Palaeozoic sediments	Late Triassic	Interval between youngest deformed rocks and oldest unconformable sediments
Gobi Basin, Mongolia	Deformation of Late Triassic sediments	209–206 Ma	Interval between youngest deformed rocks and oldest unconformable sediments
Liaoning, North China	Oblique ductile thrusting of paragneiss	~219 Ma	Ar–Ar dating of deformation fabrics
Sichuan, west-central China	Deformation on Songpan-Garz fold–thrust belt	~197 Ma	U-Pb and Rb-Sr geochronology
Longmen Shan, west China	Foreland basin deposition	227–206 Ma	Depositional ages of sediments
Fujian, SE China	Amphibolite facies metamorphism of arc rocks and terrane collision	Late Triassic–Middle Jurassic	Interval between youngest deformed rocks and oldest unconformable sediments
Peninsula Malaysia	Block collision	Late Triassic–Early Jurassic	Interval between youngest deformed rocks and oldest unconformable sediments
Vietnam/Laos	Closure of Permo-Triassic rift basins along Song-Da zone	Middle Triassic–Latest Triassic	Interval between youngest deformed rocks and oldest unconformable sediments
Kunlun Mountains, SW China	Deformation of Mazar accretionary prism and terrane collision	215–190	Syn and post deformational plutons
Central Iran	Deformation of sediments and widespread unconformity development	Late Triassic	Interval between youngest deformed rocks and oldest unconformable sediments

Ukraine	Deformation in Donbas fold belt and unconformity development	Latest Triassic	Interval between youngest deformed rocks and oldest unconformable sediments
Northern Turkey	Cimmeride deformation	215–197	Blueschist Ar-Ar ages and age of oldest unconformable sediments
<i>New Zealand</i>			
South Island	Terrane collision and metamorphism	225–170	Metamorphic cooling ages and age of oldest unconformable sediments

Table 2: Mid-Cretaceous events

Location	Event	Timing	Dating technique/criteria
<i>Antarctica</i>			
Elephant Island	Strike-slip shear on plate boundary	110–90 Ma	Blueschist Ar-Ar ages
Antarctic Peninsula	Palmer Land event and general uplift affecting arc terranes and Gondwana-margin rocks	107–103 Ma	U-Pb and Ar-Ar dating of deformation structures and syn-deformational dyke.
Marie Byrd Land	Dextral shear of crystalline basement rocks	Post ~146 Ma and pre 105–94 Ma extensional mylonite formation	Dyke emplacement timing and structural relationships
East Antarctica	Sinistral transpression of Jurassic volcanic rocks in Lanterman Range	Possibly mid-Cretaceous	Regional correlation
<i>South America</i>			
South Georgia	Thrusting of ophiolitic rocks	Aptian–Albian (125–99 Ma)	Interval between youngest deformed rocks and oldest unconformable sediments
Cordillera Darwin	Amphibolite facies metamorphism and back-arc basin closure	110–90 Ma	K-Ar dating of metamorphism.
Western South America	"Mirano diastrophic phase"	mid-Cretaceous (112–105 Ma)	Interval between youngest deformed rocks and oldest unconformable sediments
Western South America	Shoaling of basins and unconformity development	post ~111 Ma and pre Cenomanian	Interval between youngest deformed rocks and oldest unconformable sediments; dating of tuff bed.
Northern Chile	Inversion of Atacama fault zone	post ~111 Ma	Interval between youngest deformed rocks and oldest unconformable sediments
Western Peru	Mochica deformation event	Late Albian (~100 Ma)	Interval between youngest deformed rocks and oldest unconformable sediments
Western Columbia	Uplift and erosion of mid-Albian sandstones	Late Albian (~100 Ma)	Interval between youngest deformed rocks and oldest unconformable sediments
Northern Venezuela	Transpressional deformation on the Caribbean–South American plate boundary	~96 Ma	White mica and amphibole Ar/Ar ages from high pressure metamorphic rocks
<i>Central America and the Caribbean</i>			
Hispaniola	Thrust emplacement of the Hispaniola peridotite belt	Aptian–Albian (125–99 Ma)	Interval between youngest deformed rocks and oldest unconformable sediments
W Guatemala	Collision of the Chortis Block with western Mexico	125–113 Ma	Ar/Ar deformation ages from phengitic micas
Honduras	uplift and erosion of a limestone sequence	Post mid-Albian and pre-Late Cretaceous (105–99 Ma)	Interval between youngest deformed rocks and oldest unconformable sediments
Southwestern Mexico	Collision of the Guerrero Terrane	112–101 Ma	Stitching plutons showing greenschist facies metamorphism coeval with deformation
<i>North America</i>			
Southern California	Thrusting of the western Peninsular Ranges batholith	Probably 115–108 Ma and pre 99 Ma	Ar-Ar dating of deformation structures
Central California	Thrusting in Sierra Nevada	110–92 Ma with peaks at ~105 Ma and ~101 Ma	Ar-Ar dating of deformation structures
Northwestern North America	Thrusting of Coast Belt	Mid-Cretaceous (~105–80 Ma)	Interval between youngest deformed rocks and dated cross-cutting plutons
Southwest British Columbia	Thrusting of arc rocks	105–97 Ma	Interval between youngest deformed rocks and dated cross-cutting plutons
SE Alaska	Thrusting of ultramafic and arc rocks on Duke Island	Syn or Post ~108 Ma and pre ~95 Ma	Interval between intrusion of subsequently deformed plutons (111–108 Ma) and regional mid-Cretaceous thrusting
Central and northern Alaska	Widespread thrusting of arc terranes	~108 Ma	Ar-Ar dating of blueschist and amphibolite-facies metamorphism structures
<i>East and Southeast Asia</i>			
Northeast Siberia	Deformation of arc rocks in Anadyr-Koryak region	~124–117 Ma and 112–109 Ma	Ar-Ar dating of deformation fabrics
Eastern Siberia	Ophiolitic thrusting in Sikhote-Alin mountain range	~110 Ma	Ar–Ar dating of deformation fabrics
Northern Japan	Underthrusting and accretion of ophiolitic arc rocks	post ~125 Ma and pre ~110 Ma but possibly to 100 Ma	Interval between youngest deformed rocks and oldest unconformable sediments and Ar-Ar dated blueschist metamorphism

Central Japan	Metamorphism of South Kitakami and paleo-Ryoke belts	~116 Ma	Ar–Ar dating of metamorphic fabrics
Shikoku, Japan	Sanbagawa metamorphism	120–110 Ma with a peak at 116 Ma	Ar–Ar dating of deformation fabrics
Southeastern China	Thrusting of a dismembered ophiolite suite, Fujian	118–107 Ma	Age of youngest deformed plutons and Ar–Ar dating of deformation fabrics
Western China	Rapid exhumation of arc rocks	115–90 Ma	Fission track dating
Central Vietnam	Metamorphism and mylonite formation	120–90 Ma with peaks at ~115 Ma and 106–103 Ma	Ar–Ar dating of deformation fabrics
Western Philippines	Thrusting of ophiolitic rocks during block collision	~100 Ma	Interval between youngest deformed rocks and oldest unconformable sediments
Java, Kalimantan and Sulawesi	Uplift and recrystallization of high-pressure rocks during block collision	120–115 Ma	Interval between youngest deformed rocks and oldest unconformable sediments and regional correlation
<i>Australia</i>			
East and northeast Australia	Widespread erosional unconformity development in major basins	post Late Aptian–pre Early Albian (~112 Ma)	Interval between youngest deformed rocks and oldest unconformable sediments
Southeastern Australia	Folding of igneous rocks in the New England fold belt	120–95 Ma	Interval between youngest deformed rocks and oldest dated cross-cutting plutons
<i>New Zealand</i>			
South Island	Contractional deformation of arc terranes	116–101 Ma and probably pre ~110 Ma	Syn-deformational pluton emplacement and Interval between youngest deformed rocks and oldest unconformable sediments
North Island	Deformation and metamorphism of accretionary complex rocks	100–85 Ma and possibly pre ~99 Ma	Fission track dating and age of cross-cutting dykes